Computers in Biology and Medicine 87 (2017) 104–123

Contents lists available at ScienceDirect

Computers in Biology and Medicine

journal homepage: www.elsevier.com/locate/compbiomed

Simulation, identification and statistical variation in cardiovascular analysis (SISCA) – A software framework for multi-compartment lumped modeling

Rudolf Huttary [a, *], Leonid Goubergrits [b], Christof Schütte [a], Stefan Bernhard [c]

[a] Freie Universität Berlin, Dep. of Mathematics and Computer Science, D-14195 Berlin, Arnimallee 6, Germany
[b] Charité Universitätsmedizin Berlin, D-10117 Berlin, Germany
[c] Hochschule Pforzheim, D-75175 Pforzheim, Germany

ARTICLE INFO

Keywords:
Windkessel elements
Lumped models
0D modeling
Multi-compartment modeling
Cardiovascular simulation
Distributed parameter modeling
Clinical data set
Coarctation of aorta
Patient-specific models
Disease-specific models
Multiscale modeling

ABSTRACT

It has not yet been possible to obtain modeling approaches suitable for covering a wide range of real world scenarios in cardiovascular physiology because many of the system parameters are uncertain or even unknown. Natural variability and statistical variation of cardiovascular system parameters in healthy and diseased conditions are characteristic features for understanding cardiovascular diseases in more detail.

This paper presents SISCA, a novel software framework for cardiovascular system modeling and its MATLAB implementation. The framework defines a multi-model statistical ensemble approach for dimension reduced, multi-compartment models and focuses on statistical variation, system identification and patient-specific simulation based on clinical data. We also discuss a data-driven modeling scenario as a use case example. The regarded dataset originated from routine clinical examinations and comprised typical pre and post surgery clinical data from a patient diagnosed with coarctation of aorta. We conducted patient and disease specific pre/post surgery modeling by adapting a validated nominal multi-compartment model with respect to structure and parametrization using metadata and MRI geometry.

In both models, the simulation reproduced measured pressures and flows fairly well with respect to stenosis and stent treatment and by pre-treatment cross stenosis phase shift of the pulse wave. However, with post-treatment data showing unrealistic phase shifts and other more obvious inconsistencies within the dataset, the methods and results we present suggest that conditioning and uncertainty management of routine clinical data sets needs significantly more attention to obtain reasonable results in patient-specific cardiovascular modeling.

1. Introduction

Cardiovascular diseases are one of the major causes of death in the western world. One way to gain a deeper understanding of the underlying mechanisms is to simulate healthy and diseased conditions of cardiovascular blood flow by means of numerical models. Therefore, a variety of models with different levels of complexity have been proposed and established. For a very recent review, see Ref. [21].

In addition to the highly complex description of blood flow in three spatial dimensions (3D) including a fluid structure interaction (FSI) approach to model the vessel wall and fluid flow interaction, dimension reduced models with a smaller number of unknown parameters also give reasonable predictions for the mean state variables of pressure and flow in idealized vessel geometries. These models can also be employed to gain boundary conditions for higher dimensional approaches. In such multi-scale approaches, only specific areas of interest are modeled in 3D, while the rest of the cardiovascular network is described in 0D by so-called distributed or multi-compartment lumped models of blood flow, or in 1D models respectively [20,21].

Even though higher dimensional approaches allow for a more detailed description of local flow conditions, they are computationally inefficient for parameter estimation studies and have to face the so-called uncertainty problem. This is because they use numerous parameters that cannot be reliably determined from measurements, if at all. Consequently as these models can only be applied using approximate estimations or just priors for certain parameters which are not obtainable by measurement, they lead only to minor improvements in prediction of overall blood flow, as uncertainty grows with each parameter used by the model [26].

To overcome these problems, computationally efficient models with a reduced set of parameters and measurable mean quantities, such as the state variables of pressure and flow are path breaking for most simulation

* Corresponding author.
E-mail address: rhuttary@zedat.fu-berlin.de (R. Huttary).

http://dx.doi.org/10.1016/j.compbiomed.2017.05.021
Received 16 February 2017; Received in revised form 18 May 2017; Accepted 19 May 2017

purposes of the entire cardiovascular system. Furthermore, due to the large number of unknown parameters and interrelations, a single model is seldom predictive in real world problems. To approach patient-specific simulations that provide better predictions, a deeper understanding of the immanent statistical nature of the cardiovascular system is also required. Hence the "one model periodic state" approach has to be extended into a "multi-model statistical ensemble description" with distributed parameter modeling that is able to adequately describe the variety of parameters and states of the cardiovascular system in healthy and diseased conditions [33].

In a recent paper about the quantification of sensitivity and uncertainty of cardiovascular system parameters, use of the SISCA (**s**imulation, **i**dentification and **s**tatistical variation in **c**ardiovascular **a**nalysis) software framework showed to which extent certain parameters impact more on the state variables than others do [10]. A more general approach on parameter sensitivity is given in Ref. [21]. A better understanding of the dependency of model parameters on the state variables will either improve parameter estimations from measurement and/or allow for the reduction of complexity by factor fixing of less sensitive parameters [11].

To tackle the sensitivity and uncertainty problems in the cardiovascular system, a variety of software packages can be used to simulate a large number of different representations of the same modified nominal cardiovascular model in a stand-alone setting. Available simulation environments like lifeV,[1] CellML,[2] CVSim[3] [13], JSIM[4] [6], Nektar1D[5] [1] and CircAdapt[6] [3] either focus on different models and problems, or are not capable of also adequately addressing the statistical aspects of blood flow in the multi-model approach. It is, however, not enough to run simulations in some stand-alone fashion and generate data that are not, or only weakly related to a realistic distribution of parameters, and vice versa. To be able to reliably relate in-vivo, in-vitro and in-silico data for system identification, parameter estimation, validation and tracking tasks, a software framework is required that combines a highly versatile modeling environment with a high level of database integration.

1.1. The SISCA framework in short

The software framework SISCA has been developed and maintained by the Biocomputing group at Freie Universität Berlin, Department of Mathematics and Computer Science. Within the BMBF (German Federal Ministry of Education and Research) funded ForMaT (**For**schung für den **Ma**rkt im **T**eam, engl.: Research for the marketplace in team) project "information based medicine – Angio," the group's main software related objective was to develop an analytical toolbox to gain deeper understanding about the statistical aspects of cardiovascular blood flow. The software was developed to tackle a broad range of problems using fast interactive designs and workflows for multi-compartment modeling, parameter variation and case study. Validation, specifically with respect to pathological flows in stenoses, was achieved using in-vitro measurements generated by the fluid dynamical simulator MACSim[7] [24] especially designed for this purpose.

The implementation has been continuously extended towards a general multi-compartment 0D lumped modeling tool that includes nonlinear arterial wall behavior and modules for sensitivity analysis and parameter estimation. In the current state SISCA addresses:

i) Cardio vascular 0D lumped simulation on the basis of pressure/flow-coupling
ii) Stand-alone (statistical) analysis of complex arterial trees
iii) Validation of lumped model based description and parameter estimation using in-vivo and in-vitro measurements.

Current development objectives are:

i) Parameter estimation and model inversion on the basis of the Unscented Kalman Filter and the Bayesian inverse problem (BIP)
ii) Interfacing with other simulation environments
iii) Pressure/flow-coupling in multi-model settings and multi-scale approaches.

The software framework SISCA is entirely written in MATLAB[8] by use of native OOP design. It provides an expandable collection of components that address a variety of modeling, signal processing and simulation tasks based on solid database storage. The most notable features are:

- inferring and solving large systems of ordinary differential equations (ODE) from interactively composed and parameterized models;
- statistical analysis by Monte Carlo simulation scenarios;
- parameter estimation;
- system identification and
- data and signal conditioning and visualization.

To be able to maintain a large stock of modeled structures, parameter sets, simulation runs and result sets, SISCA uses MySQL as its main persistence layer. This approach guarantees that all data and relations between models, parameters, measurements and simulation runs may be stored for permanent availability and further analysis in a database with referential integrity and extensible design. The current version of the framework comprises bridges to include in-vitro or in-vivo measurements for simulation tasks, e.g. for system identification, state and parameter estimation, parameter tracking and sensitivity analysis. It has been – and is – actively developed and used for several research projects and doctoral theses at the Freie Universität Berlin and the University of Applied Sciences Pforzheim.

2. Methods

Within this section, we discuss the Windkessel approach and its embedding into general multi-compartment lumped models. With respect to the implementation of the software framework presented in the following section, we show how state space representation can be used to map component-oriented design and introduce additional model types that lead to more complex and sophisticated multi-compartment models and simulation scenarios.

2.1. Windkessel models

Originally introduced by O. Frank [9] more than a hundred years ago, the Windkessel model (WKM) exploits the hydraulic-electric analogy to describe the pulsating arterial blood flow in terms of electric notions.

[1] lifeV is an open source OOP library for the numerical solution of partial differential equations with the finite element method. Implemented in C++ by the CMCS at EPFL in Switzerland, the MOX at *Politechnico di Milano* in Italy and REO group at INRIA in France.

[2] CellML is being developed as part of the Physiome project, founded by P. Hunter, University of Auckland, NZ. It focuses on multi-scale modeling of organs and organ systems, based on model encoding standards.

[3] CVSim is a lumped-parameter model of the human cardiovascular system developed for research and teaching at MIT and Harvard Medical School.

[4] JSIM is a Java-based simulation system for building quantitative ODE and PDE numeric models and general analysis with respect to experimental reference data and is part of the worldwide Physiome project.

[5] Nektar1D is numerical code for solving nonlinear 1D equations of blood flow in arterial networks; headed by Jordi Alastruey at King's College, London.

[6] CircAdapt is real-time simulation environment for study of cardiovascular system dynamics in a wide variety of physiological and pathophysiological situations. Developed in MATLAB, it was released as freeware by the CircAdapt Research Team based at the Department of Biomedical Engineering, CARIM School for Cardiovascular Diseases, Maastricht University Medical Center.

[7] MACSim (Major Arterial Cardiovascular Simulator) is a full sized mock circulatory system with multipoint sensor measurement comprising an artificial heart and 33 main arteries.

[8] by The Mathworks.

Over time, the once simplistic two-element model has been broadly adopted and stepwise improved and refined. At present mainly linear three and four-element formulations of the WKM are considered by authors, while numerous more elaborated approaches addressing more specific issues exist as subtypes – e.g. visco-elastic models (Voigt, Maxwell), distributed or multi-compartment models [20], and transmission line models [31]. The four-element WKM, characterized by also accounting for inertial effects, splits into a serial (W4S) and a parallel (W4P) scheme, each having its pros and cons [5,20,27,32].

The present paper mainly refers to the W4S scheme as shown in Fig. 16 and Fig. 3. Readers who are not familiar with four-element WKM will find a mathematically more detailed introduction in Appendix A.

Beyond formal criticism, the WKM – in all its manifestations – has been discussed controversially for many other limitations. Especially when it comes to accounting for wave travel and wave reflection, and with respect to frequencies exceeding heart rate, the model's scope exhausts [29]. After all it seems impossible to set up a model as simple as the Windkessel model that also accounts for wave reflections that are not only caused by an actively regulated arterial structure, but also by surrounding tissues, muscles, muscular activity, bones and organs.

Nevertheless, the Windkessel framework is a powerful approach to obtaining reliable and efficient simulation results for pressure and flow calculations at a coarse level with only a minimal set of basic parameters that can be estimated well. It allows for lumping full arterial trees into single WKEs, as originally proposed by Frank [9], but also for a more refined multi-compartment modeling of arterial trees with respect to their dominant structures by representing segments of the main arteries with coupled WKE and lumping terminal subtrees into single terminal WKEs. A closer look at how WKE are represented will show how this can be achieved at a formal level.

2.1.1. WKE flavors

As a matter of physics, every energy-storing element in a WKE adds a dimension to the ODE system being used for description. Additionally, assumptions that have to be made for derivation lead to different (electrical) networks, depending on whether a pressure or flow boundary condition (BC) will be applied at inlet[9] and outlet [20]. Thus for each of the four possible BC pairings, different ODE systems result, which we call WKE flavors. In order to do forward calculations with a certain type of Windkessel element like the linear elastic WKE shown in Fig. 16, the correct flavor for the given BCs has to be selected. The inverted-L-network, or pq-flavor[10], consumes a pressure BC at inlet and a flow BC at outlet, while its ODE representation is derived to compute the missing flow at inlet and the missing pressure at outlet. The L-network, or qp-flavor, has exactly the reversed characteristic. With respect to multi-compartment design, each of these two flavors allows for a direct serial coupling with itself, as it computes at outlet what it expects as BC at inlet and vice versa.

Coupling a pq- and a qp-flavor formally into a combined element yields the T-network, or pp-flavor, and the π-network, or qq-flavor. For the pp-flavor the C branches and for the qq-flavor the RL branches fuse into a common branch. Due to the three energy-storing elements, their ODE systems comprise three equations. These flavors obviously allow for a symmetric and a non-symmetric setup, which we discuss below. Again, we provide further technical details in the appendices.

2.1.2. State-space representation of WKE

In state-space model (SSM), the representation of a continuous ODE system takes the form

$$\dot{x} = Ax + Bu + v \tag{1}$$

$$y = Cx + Du + w. \tag{2}$$

Equation (1) describes the state transition of a state vector x for a given control vector u introducing all BCs into the ODE system's non-homogenous part. The Windkessel parameters (R, C, L) appear in the state transition matrix A and the input matrix B. Equation (2) is used to generate the output (or observation) of the system. Matrices C, D represent the observation model allowing for mapping any combination of state and input information together into a vector y that may be used to observe the system. Gaussian noise vectors $v \sim N(0, Q), w \sim N(0, R)$ play a role when a model is used in a stochastic framework, e.g. a Kalman filter [30].

Discretization turns the equation system (1), (2) formally into

$$x_{k+1} = A^d x_k + B^d u_k + v \tag{3}$$

$$y_k = Cx_k + Du_k + w. \tag{4}$$

Note that discretization also affects the covariances of the noise vectors $v \sim N(0, Q^d), w \sim N(0, R^d)$.

For linear time invariant (LTI) systems, A and B are constant over time, and for simulation, a direct discretization scheme involving the matrix exponential and the transfer function approach can be used. Both allow for fast runs, provided BC are available in a batch. Solver based schemes are more flexible, as they allow for adjustable error tolerances and online (or even real time) coupling of BC, while the problem-specific right hand side function can use A and B as derived for the continuous form.[11]

Solver based schemes are also well suited for simulation of time variant systems, where A_t and B_t are time varying. They occur i) in non-linear scenarios like system identification, parameter estimation and parameter tracking, as well as ii) for non-linear WKE that contain non-linear parameters like a pressure dependent compliance C_p , or have a multi-phase definition like a lumped heart model with valves and elastance elements (Fig. 4, bottom left). Modeling non-linear effects turns the discretization of the dynamical system into

$$x_{k+1} = A_k^d x_k + B_k^d u_k + v \tag{5}$$

$$y_k = Cx_k + Du_k + w. \tag{6}$$

We cover the state space representation of the four flavors of a linear elastic WKE in more detail in Appendix B.

2.2. Multi-compartment modeling and interfacing

From equation (1), it should be clear that the general setup for a 0D lumped model simulation with pressure/flow coupling requires a fully parameterized derivation and known BCs at inlet and outlet. The idea behind multi-compartment 0D modeling of arterial trees is to arrange compatible flavors of lumped models into a structure, with inlets and outlets coupled appropriately in the sense that BCs are formally either settled by the state of their predecessor and successor compartments or by BCs of the full tree.

When some indexing scheme is introduced with index variable $i \in \{1, \ldots, n\}$ that enumerates a tree with n compartments C_i, then each node represents a fully parameterized lumped model. As the equations of each compartment enlarge the ODE system, the tree's state-space A matrix turns into

[9] "Inlet" and "outlet" are related to the main flow direction. Other authors [20] use instead "proximal" and "distal" to underline the loss of locality in the context of lumped models.

[10] We name flavors by their BC at inlet and outlet.

[11] SISCA incorporates the mentioned direct discretization schemes, as well as a rich choice of solvers, including MATLAB solvers from the ODE and SIM families and solvers from the Sundials suite, released by Lawrence Livermore National Laboratory.

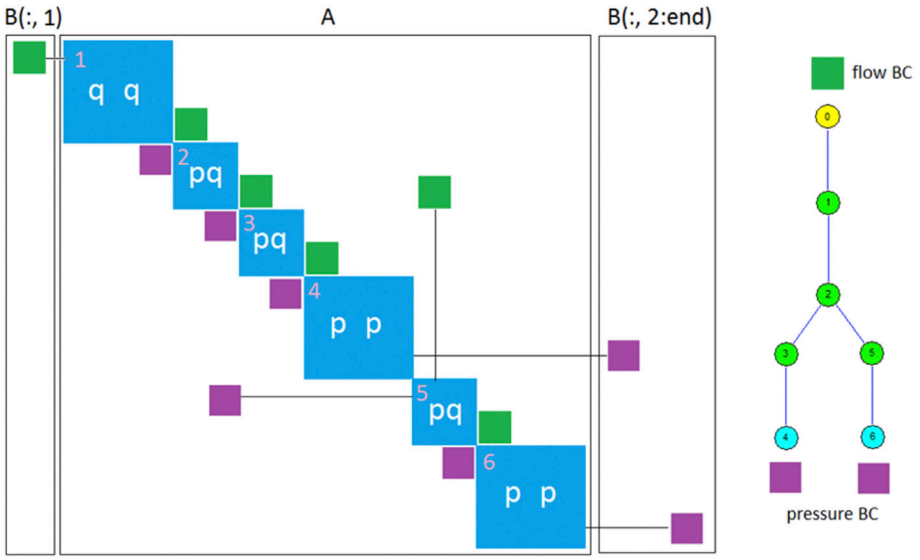

Fig. 1. Open loop multi-compartment lumped Windkessel model of a bifurcation, like a carotis. *left*: Composition scheme of the matrices used for state-space representation $\dot{x} = Ax + Bu$ of the full blown ODE system. *right*: arterial tree with nodes 1 to 6 representing lumped elements. The node with index zero is a virtual node, used to represent global network parameters and to define an inlet location.

$$A = \begin{bmatrix} A_1 & \cdots & \\ \vdots & \ddots & \vdots \\ & \cdots & A_n \end{bmatrix}, \tag{7}$$

where the dominant diagonal structure is composed by the state matrices A_i of the compartments C_i. Internal coupling is achieved by placing the according entries of the input matrices B_i into A such that, according to equation (1), the computed outlet state $x_{p,out}$ of a predecessor compartment and the computed inlet state $x_{s,in}$ of a successor compartment will be the control input for any inner compartment.

To also satisfy the inlet at root and all outlets at leafs, an input matrix B is composed by the (remaining) entries of the input matrices B_{i_j}, $j \in \{i_1 = 1, \ldots, i_k\}$ of the k compartments that represent the tree's root and leaves, with $0 < k \leq n$. It takes the form

$$B = \begin{bmatrix} B_{i_1,in} & \cdots & 0 \\ & \vdots & \\ 0 & \cdots & B_{i_k,out} \end{bmatrix}. \tag{8}$$

The full scheme is exemplified for a carotid artery by Fig. 1 and can be automatically inferred for any given tree. For a more explicit discussion of this scheme with bifurcation, refer to [4].

In case of a pressure condition at inlet and flow conditions at all outlets, *pq*-flavors can be used all over to represent the tree. Nevertheless, this is not the typical simulation scenario for arterial trees. Often, a flow condition at inlet and, even more often pressure conditions at outlets, have to be modeled. While it seems straight forward to use *qp*-flavors all over, it is possible – and also has advantages for automatic inference – to use *pq*-flavors to represent all inner tree nodes and put a *qq*-flavor ahead for a flow condition at inlet, and a *pp*-flavor for each leaf node with pressure condition at outlet. Note, that parallel coupling, which is used to describe a furcation in multi-compartment design, is better expressed on the basis of a pressure BC at inlet, as this can easily be shared by multiple elements. A flow BC that is expected by a compartment with *qp*- or *qq*-flavor, would require the computation of partial flows for all branches of a furcation and is less explicit.

With inner nodes represented by *pq*-flavors, it is convenient to use a non-symmetric *pp*-flavor element for capillary tree modeling. Its resistive (RL) branch at inlet can be used to represent the artery segment geometrically, and its resistive branch at outlet to represent the capillary tree in a lumped fashion, with compliances summed up into a common compliance C. Consequently, a segment characterization based on equations (13)–(15) will only be used for the inlet branch, while the outlet branch is parameterized by characteristic R, C, L values[12] (see also Fig. 4 left).

Multi-compartment modeling is obviously a component approach. Having derived the basic state-space representations of some lumped model allowing for pressure/flow-coupling, it can be included into any compartment of a multi-compartment model with respect to flavor compatibility.

With lumped model derivation based on a set of geometric parameters including the vessel length l, some location and distance information can also be derived from the tree structure and attributed to the elements of a multi-compartment model. Hence, the scheme allows for any coarsening or refinement to be introduced at component level in a problem adequate fashion, and furthermore provides all information needed for 1D-simulation.

2.3. Result set

Solving the network equation system (3) for a discretized time interval T leads to a result set

$$X = \{x_{i,j} |\ j \in T,\ i \in \{1, \ldots, N\}\}, \tag{9}$$

where each row describes a flow or a pressure time series computed for some compartment, with N denoting the total number of equations. In a geometry-based multi-compartment model, the time series at inlet and outlet refer to different geometric locations. For instance, a *pq*-flavor has a flow calculated at its inlet location and a pressure at its outlet location (refer to equations (11) and (12) and Fig. 16), and a *pp*-flavor has a flow calculated at inlet and at outlet plus a pressure at its internal coupling location. Obviously, the ordering of p and q type equations depends on how the structure is modeled (Fig. 1) and how the tree is enumerated.

The inlet and outlet time series computed for a compartment in fact

[12] For vessels with small radii, inertial effects can be neglected. Depending on the setup, capillary compliance is also often neglected. Peripheral resistance in turn plays a dominant role, because it is responsible for almost all pressure drop in the system.

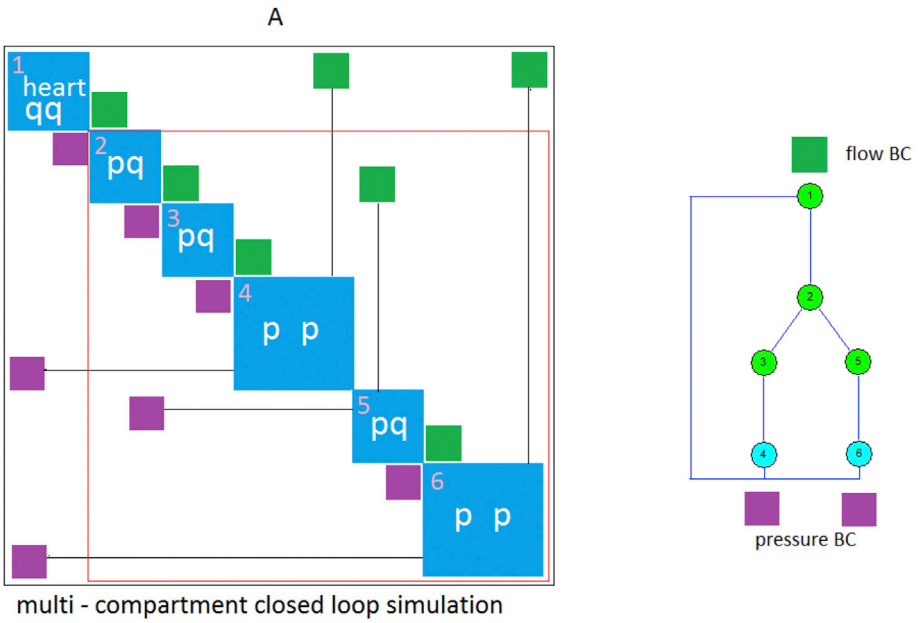

Fig. 2. Closed loop multi-compartment lumped Windkessel model set up around a bifurcation structure containing a lumped heart model at node 1. With all outputs and inputs coupled internally, the state transition rule reduces to $x_{k+1} = A^d x_k$.

refer to distinct locations. To achieve a unified observation perspective that attributes a pressure p_k and a flow q_k time series to each location $k \in \{0, \cdots, n\}$ represented by a node in the structure, an observation vector $Y = \{y_{i,j} | 0 < i < 2n,\ j \in T\}$ can be calculated. This involves some reordering of equation indices and summing up partial flows at furcation points, so that pressures and flows referring to the same location are paired properly. Thus, with locations represented by nodes, the edges represent the vessel geometries leading to these locations. In equation (4) this is formally expressed by applying matrix C to the state vector. To also complete this view for the (virtual) root node and each of the leaf nodes, the boundary conditions have to be mapped to their appropriate indices in observation space, which is expressed as product of matrix D and the input vector $u_i,\ i \in T$ in equation (4). For a given model structure both, C and D have to be specifically inferred.

2.4. Other model types

Pressure/flow coupling based on lumped OD models is not only restricted to linear elastic WKE. For the sake of model refinement, obviously many other types of WKE elements or related lumped models may be derived by introducing additional sub-elements, each of them being described by one or more additional parameters and arranging them into a network with pressure/flow connections [26]. In most cases, those elements may also be expressed in different flavors as discussed previously in this section.

2.4.1. Visco-elastic WKE

Good examples for model refinement are the two visco-elastic types shown in the top part of Fig. 3. The visco-elastic Voigt model is derived from a spring-dashpot mechanical equivalent and introduces an additional damping resistance in series with the compliance.

In contrast, the visco-elastic Maxwell model uses the electric analogue of the Maxwell-Wiechert model, also known from mechanics. With this approach, the damping characteristic is modeled in more detail by introducing two additional RC parallel circuits in series with the main compliance. Consequently, the *pq*-flavor of a Maxwell WKE has four additional parameters – two of them represent energy storing elements. It requires four equations to describe its state (*qq*-flavor extends this number to seven) and its state-space representation is:

$$A = \begin{pmatrix} \frac{-R}{L} & 0 & 0 & \frac{-1}{L} \\ \frac{1}{C_1} & \frac{-1}{C_1 R_1} & 0 & 0 \\ \frac{1}{C_2} & 0 & \frac{-1}{C_2 R_2} & 0 \\ \frac{1}{C} + \frac{1}{C_1} + \frac{1}{C_2} & \frac{-1}{C_1 R_1} & \frac{-1}{C_2 R_2} & 0 \end{pmatrix}, \quad B = \begin{pmatrix} \frac{1}{L} & 0 \\ 0 & \frac{-1}{C_1} \\ 0 & \frac{-1}{C_2} \\ 0 & -\left(\frac{1}{C} + \frac{1}{C_1} + \frac{1}{C_2}\right) \end{pmatrix}. \tag{10}$$

In this system, the second and third equations describe a subspace solely responsible for internal state retention, while the states used for pressure/flow coupling at inlet and outlet result from the first and last equations.

2.4.2. Heart WKE

Another more complex model type, essential for closed loop modeling of blood circulation, is the two-chamber heart element (Fig. 4, bottom). As discussed in more detail in Ref. [8], this model (partly) has some non-linear characteristics, as it incorporates two valves, electrically modeled as diodes and a triggered time dependent ventricle volume E, modeled by a parameterized elastance function. All three are non-linearly dependent on pressure conditions at inlet and outlet.[13]

It is straightforward to turn the scheme for open loop operation defined by the equation system (1), (2) into a scheme for a simplistic one circuit closed loop operation, as exemplified by Fig. 2. The loop is then formally closed into a feedback loop by coupling all leaf outlets in a

[13] SISCA contains an implementation of this WKE and offers close loop simulation scenarios for it.

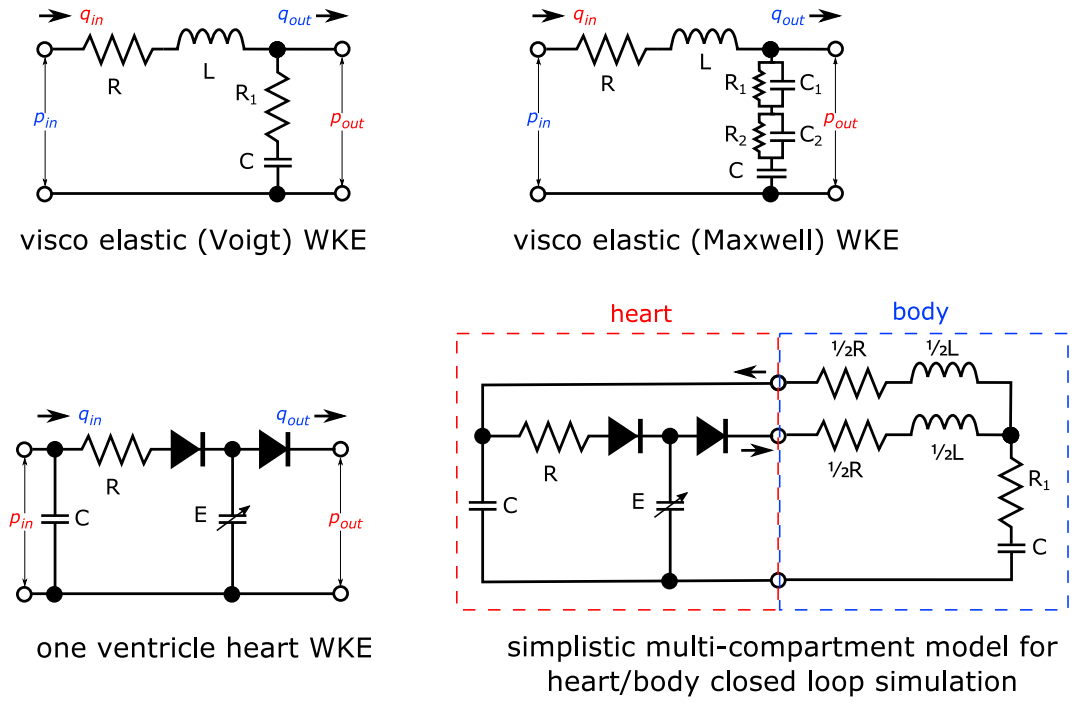

Fig. 3. Different types of WKE for heterogeneous component coupling: *top left:* visco-elastic Voigt model (*pq*-flavor, 2 equations); *top right:* visco-elastic Maxwell model (*pq*-flavor, 4 equations); *bottom left:* simplistic non-linear heart model (*qq*-flavor, 2 eq. per case, 3 different cases) with elastance (E, non-linear) for four-phase simulation (filling, isovolumic, ejection, isovolumic) and *bottom right:* circular heart/body coupling (qq, pp) for simplistic closed loop simulation.

parallel fashion with the inlet at root, so that the outlet flows of all leaf elements add up and form the flow condition for the inlet of the heart WKE at root. At the same time, the pressure computed for the heart WKE's inlet is applied to be shared by all leaf outlets. In terms of equations (1) and (8) this means that B turns into a zero matrix and all remaining B_{ij} of the leaf compartments move to the first row and first column of state space matrix A.

2.4.3. WKE types and multi-scaled models

Multi-compartment modeling based on flow/pressure coupling can further be done in colorful mixture with any variety of model types, each introducing its own parametric description, adaptiveness and – sometimes – non-linear characteristics. Examples for lumped model types with derivation from more specific descriptions are manifold and include stenosis, aneurism, anastomosis, 1D/3D coupling adapters [21], organ models (brain, heart, kidney, liver and so on), capillary trees, furcation types and so on.

With all this freedom in refining, graining and combining different model types, the multi-compartment modeling approach becomes highly versatile.

3. Implementation of the software framework SISCA and some application scenarios

After this – at least from a technical view – more general introduction to lumped models, in the following section we give a somewhat more detailed description of the technical aspects of the software framework SISCA. Implemented and maintained in MATLAB, it contains implementations of all WKE types and flavors for both operation modes (open and closed loop) presented in the previous section.

The key features of the framework are:

- fast GUI-oriented workflows to interactively:
  a. design, build and parameterize multi-compartment models with arbitrary arterial tree design and refinement;
  b. run, view and analyze simulation runs for any choice of parameters and boundary conditions being applied at inlet and outlet and
  c. import, view, pre/post-process and store datasets and measurements;
- a MySQL database persistency with referential integrity for all structural data, parameter sets, simulation and measurement data;
- a selection of different ODE-Solvers (MATLAB and SUNDAILS) with GUI-based invocation for
  a. simulation with interactively composed linear and (specific) nonlinear scenarios and
  b. automatic local sensitivity calculation (SUNDAILS);
- an expandable fully documented component design on the basis of MATLAB's built-in OOP support;
- a full database and view support for statistical sets and variational analysis;
- a precompiled model export for fast sensitivity analysis and parameter estimation procedures;
- a rich set of tools for data preparation, signal processing, parameter estimation and data visualization; and
- a rich high and low-level scripting interface for future code expansion and specialization.

3.1. Model designer

SISCA extensively uses MATLAB's built-in OOP support. At first glance, it offers a rich GUI based structure editor as its main front end and a layered transactional MySQL database at its back end (Fig. 8) for consistent storage of:

- model structure and design parameters;
- multiple parameter sets per structure (1:n relation);
- multiple simulation runs per parameter set (1:n relation) and
- all calculated flow/pressure relations per run (1:n relation).

SISCA's GUI-based model designer visualizes multi-compartment

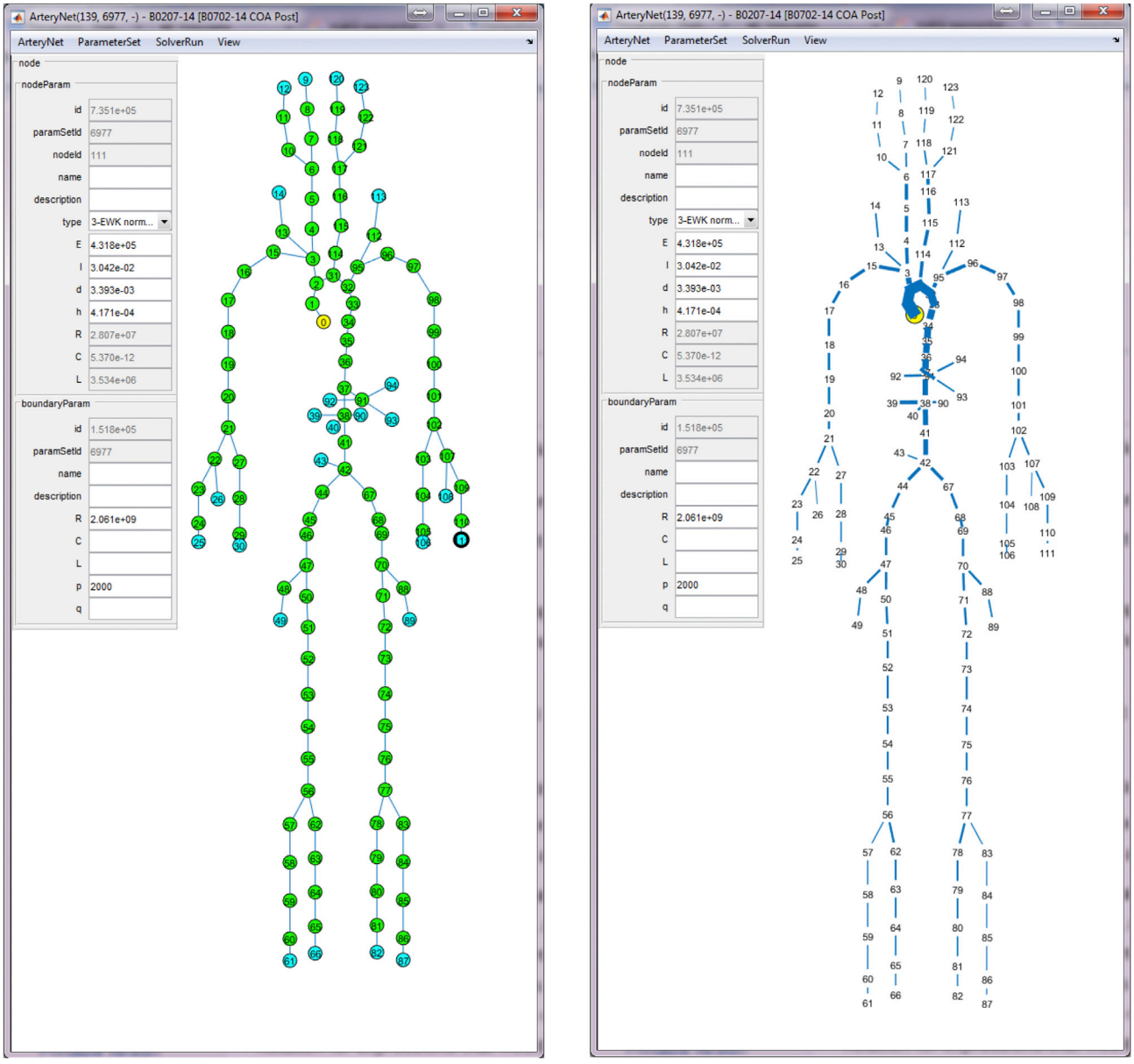

Fig. 4. Multi-compartment model of a detailed arterial tree proposed in Ref. [31] with adapted aortic structure used for the study of coartic stenosis data. The screen shot shows the full model as it is displayed in the model designer component of SISCA. *Left:* In the node edit panel on the left, the parametrization of the terminal compartment of the arteria radialis (selected node drawn bold) is displayed. *Right:* Geometrical relation view visualizes attributed lengths and radii of vessels for a fast consistency check.

models as tree structures that use a directed graph with selectable nodes and edges. Both offer context-specific operations via context menus and a parameter editor that displays when a node is selected (Fig. 4, left). To view a tree's geometry, a visualization of the metric parameters d, l is available (Fig. 4, right).

The designer component allows for:

- interactive composition, design and editing of arbitrary multi-compartment tree structures;
- visualized parametrization and editing of each Windkessel element's parameters and boundary conditions;
- running simulations with a solver, of choice and full control of time span (periodic input), resolution and error tolerance;
- persistent storage of all data and settings and
- visualizing any calculated or previously stored runs in an on-place manner by means of an interactive GUI-based viewer.

Additionally, multi-window support and copy & paste features allow for quick transfer, recombining fully parameterized subtree structures into new models and comparing multiple runs with different parameterizations and/or structures.

3.2. State-space model inference

Behind the scenes, SISCA comprises an automated model builder component that infers the state-space model (i.e. the matrices A and B) from any particular tree structure interactively modeled in the GUI based designer component, as well as for any parametrization and BC type information, by use of appropriate WKE types and elementary *pq*-, *qq*- and *pp*-flavors. R, C, L values for each compartment are computed from the more basic "primary" parameters E, l, d, h, as defined by equations (13)–(15). Additional parameters may be set in the parameter editor and also in a regularized fashion (visco-elastic types). At outlets with pressure termination, boundary resistances are integrated into the third equation by use of a *pp*-flavor, as shown in equation (19), but in non-symmetric derivation. Thus, a BC for each inlet and outlet point may be specified,

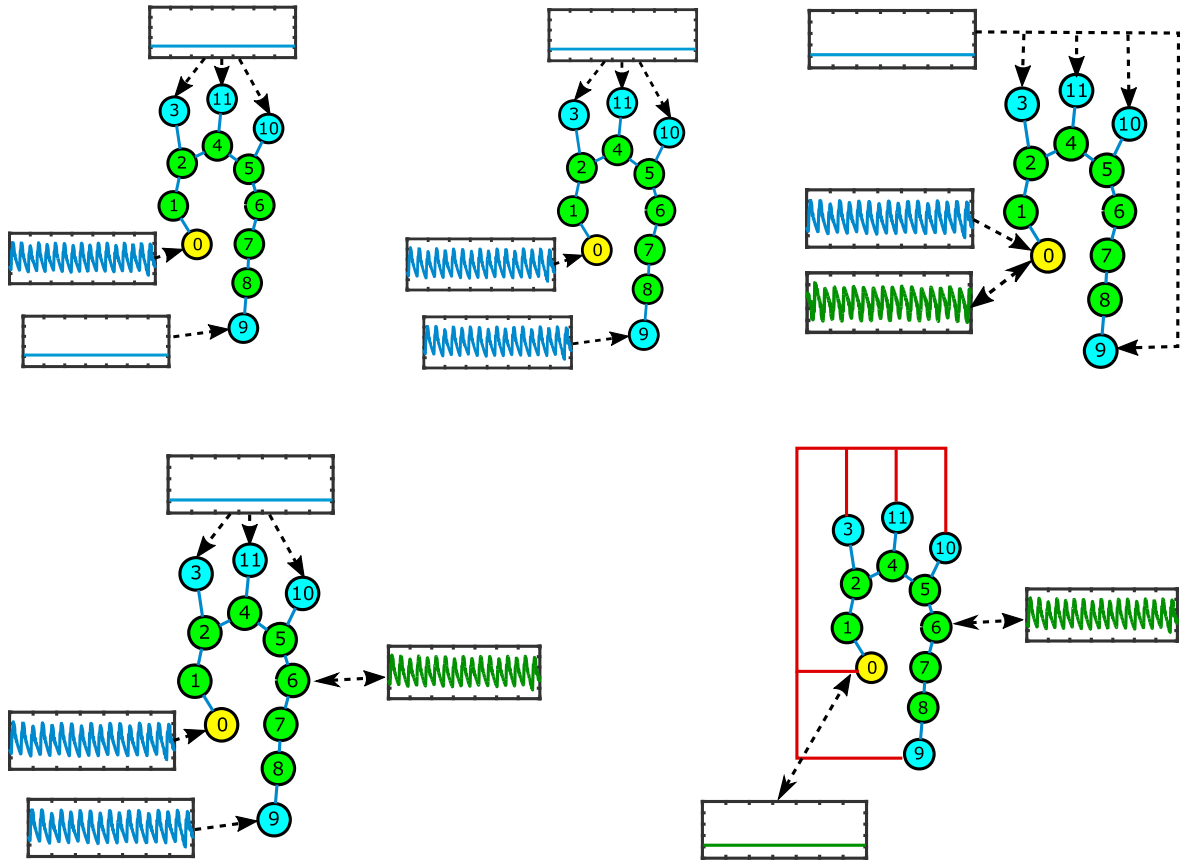

Fig. 5. Some characteristic scenarios for forward simulation and model inversion with a multi-compartment lumped model of aorta (blue/green time series indicate BC/observations). *Top left:* typical 0D-forward simulation with pressure or flow BC (blue) at inlet and all branches terminated by lumped WKE against constant venous pressure at outlets. *Top middle:* forward simulation using measurements as BC for main aorta; *Top right:* parameter estimation scheme (for system identification or parameter tracking) using a pressure and a flow condition at inlet (green), with one used as BC and the other as observation; *Bottom left:* multi-point parameter estimation scheme (only one observation point depicted). *Bottom right:* multipoint parameter fitting in closed loop setup with backflows coupled to lumped heart element at root. (For interpretation of the references to colour in this figure legend, the reader is referred to the web version of this article.)

while venous outlets are treated as special cases that are settled with constant pressure time series (of a freely specifiable level).

3.3. Interfacing

On the basis of its own OOP design, the software tool primarily offers a rich high-level scripting interface, which can be used for all sorts of console or script oriented interaction with classes, objects and data stored in database, or datatypes equipped with file readers. In seamless interlace with GUI commands this allows for incremental automation, mixed operation and interactive data analysis. The framework design is fully open to further code extension. Any integration of specific algorithms or full-grown applications can programmatically exploit or extend the structures and data in stock. Some of many examples for which specific code have already been implemented, are variation based statistical analysis of cardiovascular diseases, integration of new Windkessel elements, extraction of full blown state-space systems for speed optimized stand-alone parameter estimation, medical device development, solver palette extension, parameter sensitivity analysis, multi-model coupling, data integration, mixed non-linear and linear simulation (see Fig. 7).

3.3.1. Interface documentation

Information about class and object design for scripting interface usage is fully integrated into the native help system of MATLAB. At class and instance level, it covers all properties and methods meant for external use, while providing specific details on all parameters and giving typical examples for possible calling and usage.

3.4. Sensitivity analysis

Simulation runs can, also at GUI level, be extended selectively with respect to each segment and main parameter (R, C, L …) to additionally compute local sensitivity analysis data, provided a solver from the SUNDAILS suite is used. Additionally global sensitivity methods and calculation scenarios have been implemented for selected structures on the basis of the scripting interface and used for sensitivity studies [5,11,12,34].

3.5. Simulation scenarios

From a formal point of view, multi-compartment model design can be done at any (reasonable) refinement and tree structure. SISCA contains built-in support for a broad range of simulation scenarios covering simple two node designs as well as multi-furcation structures up to full arterial trees of humans, animals or in-vitro simulators like the Major Arterial Cardiovascular Simulator (MACSim) [24]. At a refinement level proposed by Westerhof et al. [31], who modeled and validated the human arterial tree with 121 segments by use of analog computing devices, the parametric description of the multi-compartment model will comprise more than 500 parameters and its dynamics more than 250 ODEs, depending, of course, on the WKE types used (Fig. 6).

3.5.1. Open loop simulation

Classical (open loop) setup for forward calculation in arterial flow simulation assumes a constant (venous) pressure at all outlet nodes, thus requiring only one measured time series to be applied as BC at inlet

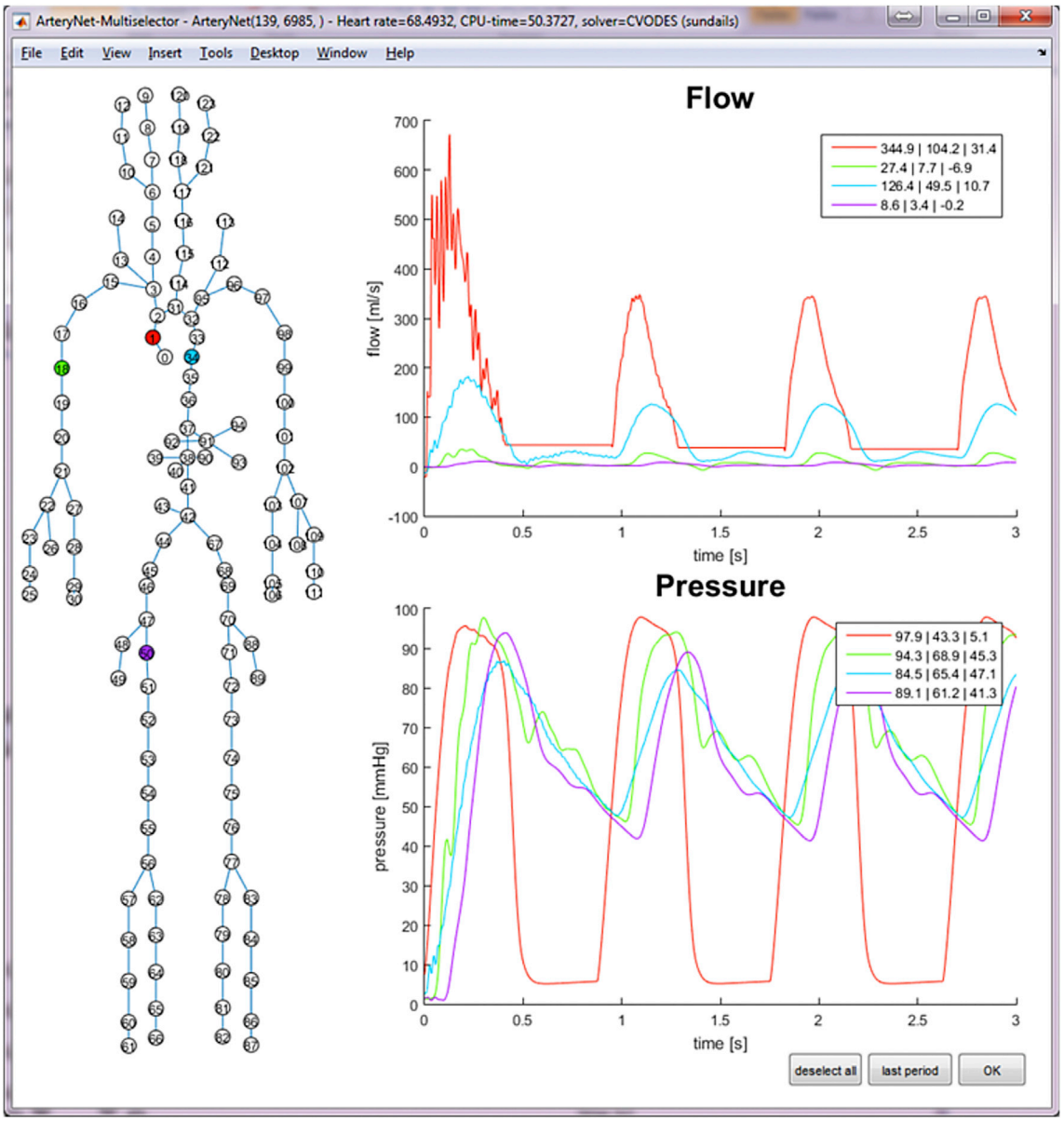

Fig. 6. SISCA's result viewer selectively displaying the result set of a closed loop simulation at left ventricle, a. desc. a. femoralis and a. brachialis during interactive setup while modeling coarctation of aorta by use of a lumped two chamber heart model, see also: Fig. 5, bottom right. With unknown initial value the simulation needs about one full cycle until the state converges into a periodic solution.

(Fig. 5, left). For this scenario, it is also common to model terminal WKE using a boundary resistance against a fixed pressure level (usually 0 mmHg). In SISCA, however, terminal nodes with pressure BC are more generally represented by full blown pp-flavors, which allows for easily reducing full models to partial structures and vice versa, as well as the application of measured pressure and flow time series at both inlet and outlets (Fig. 5, mid). Therefore, any constant pressure level (or flow) can be specified at any outlet.

Non-linear simulation scenarios on the basis of an own WKE model derived for the identification of pressure-dependent compliance C_p have also been implemented, tested and investigated by one the authors in the course of the BMBF funded project KF2698702KJ1 "Development of a non-invasive blood pressure measurement device."

3.5.2. *Closed loop operation*

Further, closed loop operation has been implemented and tested at a formal level, but not studied extensively so far. Automated state-space model inference currently takes the path that the first node is automatically converted (overridden) into a heart compartment, having its inlet directly connected to all outlet points (Fig. 5, right), as discussed in more detail in the previous section. The integration of more detailed, lumped, four chamber heart models is planned.

3.5.3. *Task preparation*

For designing, initializing, maintaining and harnessing complex multi-compartment models in order to successfully mimic and analyze specific cardiovascular scenarios on the basis of in-silico simulation runs, a software tool cannot be versatile enough. At GUI level, only a subset of an infinite number of tasks can be anticipated and fully formalized. But others, not fully covered, can at least be prepared and supported. By its OOP design, SISCA reflects any changes made at GUI level at command line and scripting level and vice versa. For common tasks like querying the tree, regularized re-parametrization, solver preparation and invocation, a rich set of high and low-level interface functions can be used. This allows for individual workflows composed by

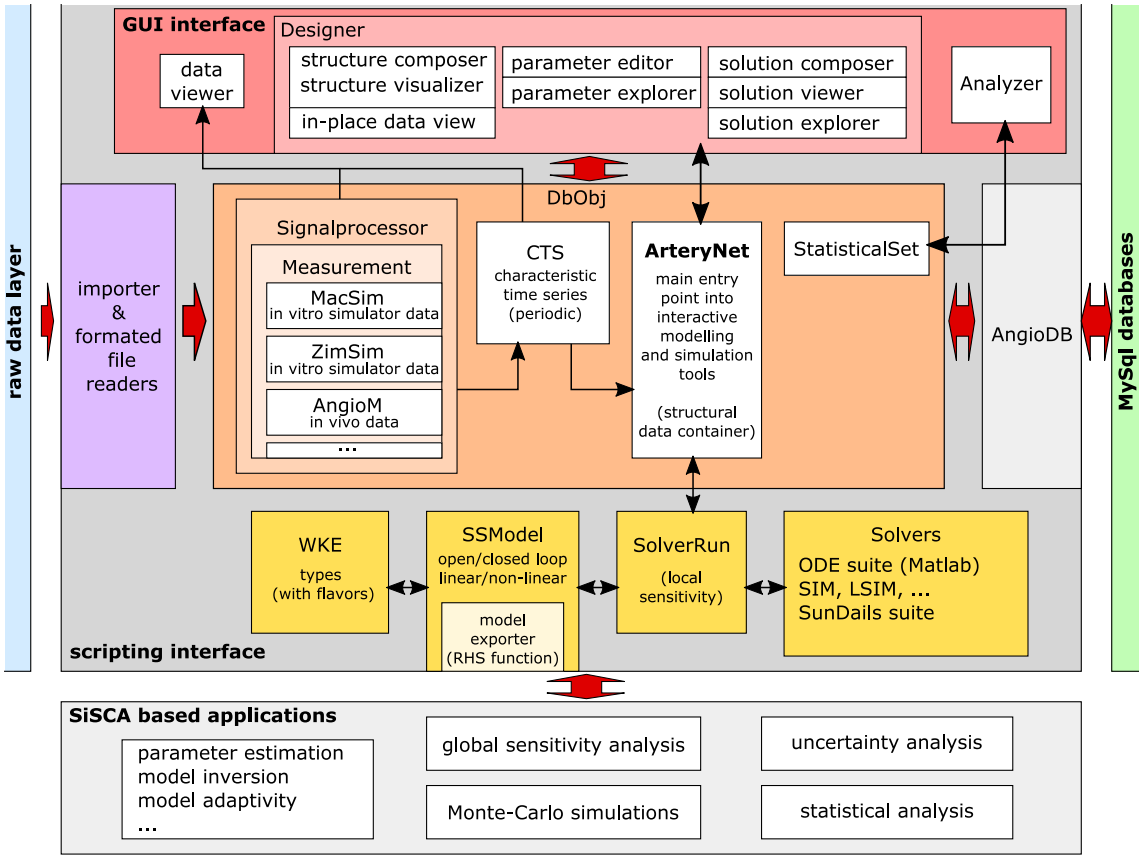

Fig. 7. Main components and architecture of the SISCA application in overview. The core components and classes of SISCA's OOP design are grouped in the central gray box and layered by their tasks. Raw data import and conditioning is specifically handled by classes derived from *Signalprocessor*. Main entry point of the application into the GUI oriented modeling and simulation environment is *ArteryNet*. All data, raw data, conditioned data, interactive model designs, parameter sets and any result sets of *SolverRun* objects can be persisted to a MySQL database. While SISCA specifies several interfaces to facilitate scripting with its main objects, all its classes and objects expose data and methods through public interfaces and may be accessed by SISCA based applications through the generic scripting interface of MATLAB.

i) any mixture of partial automation and interactive steps offered at GUI level,
ii) any combination of GUI build-in visualization with supplementary plotting tools and output,
iii) any combination of data natively stored in database and data from external sources.

To also address the dark side of versatility - longer execution times - SISCA allows for symbolic code output for right hand side functions of automatically inferred state-space systems from interactive design or database stock at its scripting level. This code can easily be included or ported into any other framework or application for stand-alone and fast computation in complex scenarios like, e.g. Monte-Carlo simulation setups, global sensitivity calculation or parameter estimation frameworks.

3.6. Variational statistical analysis

One of the main objectives for SISCAs implementation was distributed parameter sampling and result viewing for any given model and parametrization. From an OOP perspective, the solution was

i) to implement a *StatisticalSet* object that relates a primary *ParamSet* object describing a nominal parametrization (expectation value) for a given structure (*ArteryNet* object) with a collection of *ParamSet* objects compiled by a sampling scheme like Monte Carlo on the basis of a multivariate distribution for the parameters variated,
ii) to allow for simulation runs upon this set to be persisted to database (Fig. 8) with full context retrieval for further analysis.

While sampling schemes and distributed calculation for a given nominal parametrization may be freely scripted with MATLAB language, a *StatisticalSet* object provides all necessary operations for simulation and persistent storage as part of SISCA's scripting interface (Fig. 7).

For fast result analysis, a viewing tool, with a high level of interactive control was implemented. It selectively retrieves and displays information on the runs using "horizontal" access to some or all result sets at node or node difference level, as shown in Fig. 9.

4. Modeling and validation with routine clinical data

Parameter estimation has many faces. Solutions and validation heavily depend on the availability and quality of data and the number of parameters to be estimated. One of its most challenging faces in cardiovascular modeling and analysis is that it commonly has to be based on a very small footprint of available clinical data for cost, systematic and (very important) ethical reasons. According to [26], the most obvious challenges are:

> *"The invasive nature of many of the measurements, restricted access to the required measurement sites due to anatomical configuration, practical difficulties in the orientation of flow probes (particularly invasive ones), sometimes difficulties in synchronization of pressure and flow data (particularly when not measured simultaneously), limited precision in the pressure/flow sensor".*

However, in routine clinical context additional difficulties arise from (partially) conflicting measurements with unknown or fuzzy circumstances and preprocessing, records with weak time correlation (e.g.

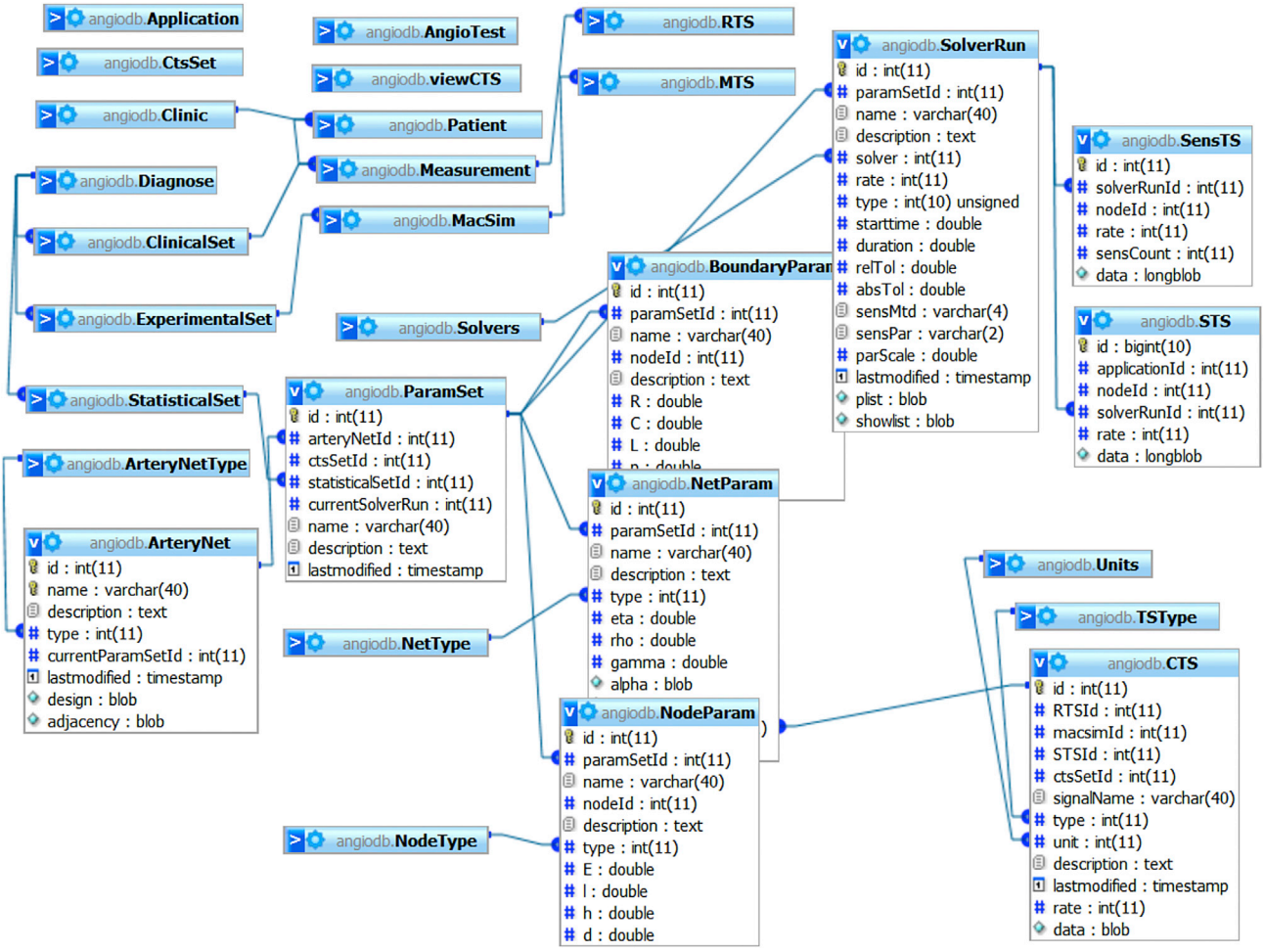

Fig. 8. Current MySQL database design (partially unfolded) used by SISCA. Transaction based referential integrity is enforced by use of the InnoDB engine.

composed under the assumption of autocorrelation as in 4D flow MRI, or even distanced over very large time gaps), and incomplete meta data. In this case many additional assumptions come into play that have to be weighed and set into relation with common (prior) knowledge and statistics. To receive a measure of the quality of such an optimal solution, uncertainty quantification comes into play as an essential validation component.

Patient specific modeling is confronted with all those problems and has to adequately deal with them. As part of a preliminary study on the usability of routine clinical data for the fitting of multi-compartment lumped models, SISCA has been used to conduct patient specific modeling for some clinical data sets. In the following section, a specific clinical data set with some of its idiosyncrasies is presented, possible simulation scenarios are identified and a method for modeling a before and after scenario based on the inherent multi-compartment approach of SISCA is developed.

4.1. Patient specific modeling – a case study on coarctation of aorta

The clinical data set presented was collated from a patient (13 years old, 148 cm, female) diagnosed with coarctation of aorta (CoA). This is a severe congenital heart disease causing upper-body systolic hypertension and lower-body hypotension [16]. The patient was treated by an endovascular stent since the Doppler echocardiography based pressure drop ($dp = 4 \cdot V_{max}$, where V_{max} is the maximal velocity magnitude through the stenosis) exceeded 20 mmHg. Local Institutional Review Board approval was obtained and informed consent was given by the patient.

4.1.1. The data set

Clinical data including MRI acquisition data were collected before and after the treatment procedure in the Department of Congenital Heart Disease and Paediatric Cardiology at the German Heart Institute in Berlin. MRI examinations were performed on a whole-body 1.5 T MR scanner (Achieva; Philips Medical Systems, Best, The Netherlands). A five-element cardiac phased-array coil was used for signal acquisition.

The full clinical data set comprised:

1. A set of metadata mainly including information about the patient's age, gender, body size and body weight, as well as cuff pressures (systolic and diastolic) on arms and legs before and after treatment (during MRI acquisition). Cuff pressures were assessed by using Dinamap Pro 300V2 (GE Medical Systems, Fairfield, CT, USA).
2. A set of selected invasive (catheter) multi-point (left ventricle, ascending aorta and descending aorta) pressures in-sync with ECG, in pairwise recordings (simultaneous pressure signal acquisition at the catheter port – femoral artery) with full time, however weak location information was recorded during cardiac catheterization. Cardiac catheterization was done under control with conventional x-ray angiography with Philips Allura Xper FD 10/10 (Philips Medical Systems, Best, the Netherlands) using an injection of a contrast agent (Ultravist, Schering, Berlin, Germany).
3. A set of flow rates derived from four-dimensional velocity-encoded MRI (4D-VEC-MRI) with large time gaps pre (57 days) and post (6 months) treatment. The routine protocol for this involved using an anisotropic 4D segmented k-space, phase-contrast gradient echo sequence with retrospective electrocardiographic gating without

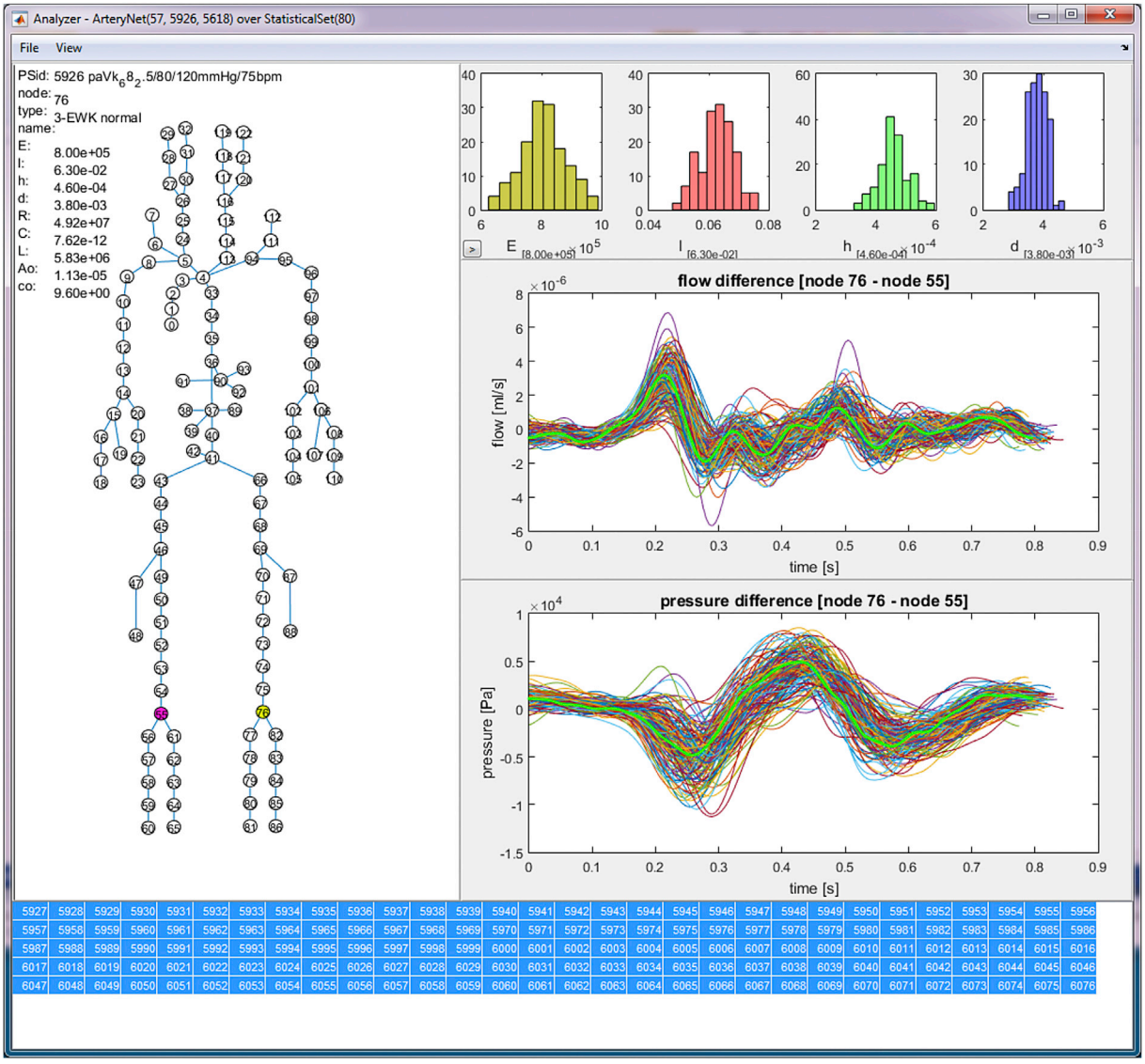

Fig. 9. Viewing a Monte Carlo simulation of a peripheral artery occlusive disease scenario in the *Analyzer* tool. The presented snapshot shows a variational multi-signal plot of the signal differences between two (in-place) selected nodes based on a set of 150 runs (each selectable in bottom panel), with nominal signals plotted in bold green. Parameter statistics of the displayed statistical set is shown in the top right panel (secondary parameters available per scroll). Values of each parameter of each run for the selected node may be retrieved and displayed per mouse click upon the corresponding plotline. (For interpretation of the references to colour in this figure legend, the reader is referred to the web version of this article.)

navigator gating of respiratory motion, in order to minimize acquisition time. The sequence parameters were: 30 slices, with an acquisition resolution of 2.5 × 2.5 × 2.5 mm, reconstructed voxel size of 1.7 × 1.7 × 2.5 mm, repetition time 3.5 ms, echo time 2.2 ms, flip angle 5°, 25 reconstructed cardiac phases, velocity encoding 4.0 m/s and the number of signal averages 1. High velocity encoding (3.0 m/s) in all three directions was used in order to avoid phase wraps in the presence of stenosis forming complex 3D flow. Flow data sets were quantified with GTFlow 1.6.8 software (Gyrotools, Zurich, Switzerland). Flow rates in the ascending aorta just above the sinotubular junction and in the descending aorta (behind coarctation) at the level of the heart apex were evaluated.

4. An end-diastolic geometry was derived from a navigator-triggered whole heart (3DWH MRI) sequence. The sequence parameters were 76 slices, with an acquisition resolution of 0.66 × 0.66 × 3.2 mm, reconstructed voxel size of 0.66 × 0.66 × 1.6 mm, repetition time 4.0 ms, echo time 2.0 ms, flip angle 90°. Based on the slices, geometrical reconstruction of the CoA using the software ZIB-Amira (Zuse Institute Berlin, Germany) was conducted. First, raw data were resampled to the isovoxel size of 0.7 mm × 0.7 mm x 0.7 mm using the Lanczos filter. Then, level-set segmentation techniques [25] including voxel labeling with subvoxel accuracy using thresholding in combination with region-growing techniques [19] were used. The final label field was transformed into a triangulated surface using a Marching Cubes algorithm [17]. The surface was then smoothed using the Laplacian algorithm. The smoothing was done to remove surface mesh artifacts. The resulting surface mesh was exported into STL file format for further processing.

4.1.2. *Looking at the data – identifying possible tasks*

In a first step the available meta-information on the clinical data set was evaluated and some analysis was done to identify

i) any mismatches and inconsistencies within the data set with respect to coherence, and
ii) a number of possible simulation scenarios for which an 0D multi-compartment model could be set up and used for parameter estimation and model fitting.

Even if data was recorded with professional care and by use of state of

Table 1
In mixed data sets consistency, quality and coherence of measurements are challenging problems and demand explicit modeling and quantification of comparability and uncertainty.

No.	Identified problem and its cause	Modeling task
1	Large time gaps between recordings of pressure and flow must not be neglected. The patient's physiological conditions during surgery and MRI acquisition strongly differ. The system was "changed" due to surgery.	uncertainty and comparability of measurements
2	Time scale in sampling of flow and pressure differs by factor 15. Flow is effectively calculated at a rate of 33/s, pressure at 500/s. Strong coupling in simulation is not possible because of 1).	address different time scales
3	Cuff measurements significantly (>25 mmHg) differ from invasive pressures at systole (see Table 2). Possible reasons: surgery context, pharmaceutical impact, sensor calibration. Also left/right cuff pressures taken during pre-surgery MRI sessions significantly differ at legs and arms.	uncertainty from inconsistent data sets
4	Catheter was moved while recording. Location information is poor or missing. Location can only be read coarsely from the data.	uncertainty of wave form by catheter location
5	Any multi-point measurement being reconstructed from paired catheter measurement underlies the autocorrelation assumption. Synchronization information is derived from ECG signal only. While pulse rates slightly vary, also the influence of breathing is not taken into account.	uncertainty induced by ECG triggered remodeling of pulse form
6	Catheter is a significant obstacle and its location has impact on measured data.	uncertainty induced by catheter disturbance
7	Phase shifts of catheter pressures due to pulse wave velocity in pre and post treatment data seem unrealistic (Fig. 13, left). While large phase shifts can be seen in pre-treatment data, in post-treatment data, the distal pressure wave almost seems to be in phase or even overtake the proximal.	correction of phasing errors
8	In post-treatment data, relative pressure offset within pairs seems unrealistic and indicates a calibration issue. Diastole at distal locations should not exceed diastole at proximal locations.	correction of offset errors

the art equipment, strong correlation of the different data within such a data collection cannot be expected due to significant situational differences (MRI session versus surgery under general anesthetic) and large time gaps between the sessions in which the recordings were made. Table 1 gives an overview of the paramount discrepancies.

4.1.3. Identification of possible simulation scenarios

Fig. 10 provides some overview of the measurements and their locations contained in the clinical data set. It is obvious that those locations play an import role for model setup, because measurements can be used either as BC at inlet and outlet points, or as observational feedback for adaptive model fitting schemes operating upon some cost function. Parameter estimation schemes based on the variational approach evaluate a functional over a simulated time period (e.g. over one or several pulse waves) to compute an optimal parameter set for reproducing the data in a minimized error fashion with simulation runs upon the model of choice. While this approach works well for system identification in many setups, especially when coherent data sets and adequate models are available, it leads to a second estimation problem. This second issue is connected with the difficult task of finding a functional that accounts for uncertainty and conflicting information in the context of multi-objective optimization when the data is not well synchronized, incoherent or even corrupted.

Estimation schemes based on stochastic methods that solve the Bayesian inverse problem within some more or less history reduced setting, like the Kalman filter, bring their own uncertainty calculus [23]. The price is that they impose certain assumptions on the probability distribution of the data and expect full prior information in the form of covariances, which have to be specifically composed in a problem related form.

Therefore, when it comes to accounting for uncertainty, it should not be surprising that any optimized set of parameters in a modeling scenario heavily depends on the priors chosen for the setup of the estimation scheme. Table 1 gives a short overview of the issues that have to be covered by uncertainty modeling.

The full pre-treatment pressure record shown in Fig. 11 mainly contains a left ventricle (LV) sequence lasting about twelve seconds, an ascending aorta (ASC) sequence lasting about 35 s and a descending aorta (DESC) sequence lasting about twelve seconds. These sequences are paired with i) pressures recorded at the arteria femoralis (FEM), where the catheter was inserted for surgery access, and ii) ECG signals providing some reasonable synchronization information for autocorrelative evaluation. Fig. 13 shows the available record of post-treatment pressures, containing only an ASC and a DESC sequence, but no LV sequence. For more detail, some characteristic periods of pre and post-treatment pressures at ASC and DESC and their pairing with FEM are shown in Fig. 13, left. Note that with respect to pulse wave velocity analysis, the phasing between DESC and FEM seems to be unrealistic at least in the post-treatment data.

The corresponding pre-treatment flows shown in Fig. 13 were recorded almost two months before the surgery. Thus they can only be used as a rough lead to estimate some systemic and heart parameters, including elastance function parameters and mitral resistance. A possible setup for this would be a multi-compartment lumped model containing a heart element and at least the major aortic structure, see Fig. 5, or even better, a full arterial tree also covering the cuff measurement points as shown in Fig. 10 and the catheter's port sensor at FEM for further analysis (also see Ref. [28]).

In the following sections, we identify and sketch some possible setups. Depending on the research interest, they can be easily addressed and studied interactively by use of SISCA to prepare and accomplish model fitting and parameter estimation tasks based on a typical clinical data set similarly composed as the one presented in Figs. 10–15 and Tables 1–3. Also, refer to Fig. 5, which depicts the most prominent use cases in the example of a multi-compartment setup for the major aortic structure.

4.1.3.1. With linear WKE model. In the retrospective case with post-treatment data already available, it seems easier to identify a parametrization of the "healthy" condition model first. This can then be built upon when fitting the pathological condition of the model, as it requires more explicit modeling. Practically, best results are obtained when both tasks are tackled in an interlaced fashion. The more regard given to information about the system, the better the results will be.

The following procedure describes the main steps that were conducted to gain a patient-specific model upon the said clinical data set attributed to a 13-year-old female with a body height of 148 cm and diagnosed with CoA. The task was approached by fitting a linear multi-compartment lumped model of high detail, comprising 123 WKE of type visco-elastic Maxwell as characterized by Equation (10) and Fig. 3, top right.

1. **Start with a healthy condition model and a validated (!) standard parametrization:** For the specific case study, the standard model presented in Ref. [31] and depicted in Fig. 10, left, with some minor changes concerning aortic segmenting and WKE type, was used as a starting point. Note that the compartment parameters fully stated in Ref. [31] refer to a male adult with a body height of 175 cm.

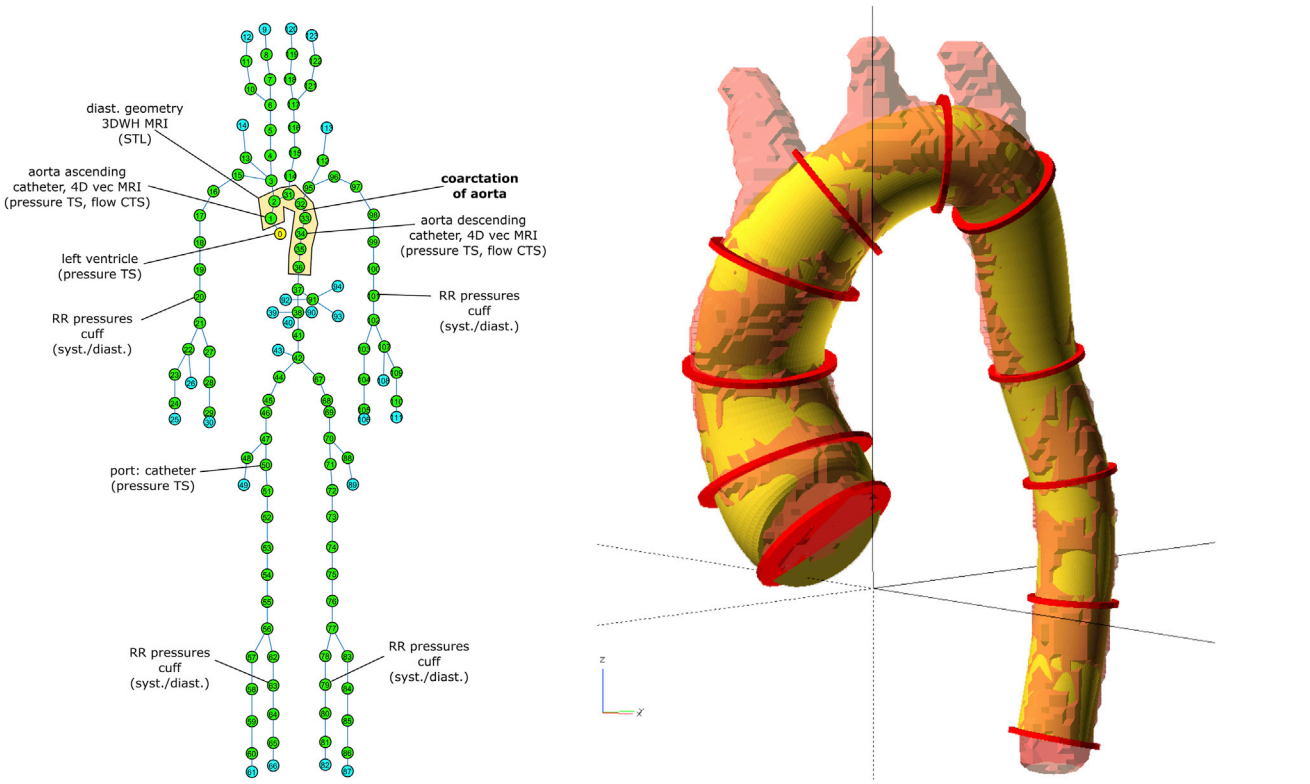

Fig. 10. Available clinical data in overview. *Left:* overview over all available data and locations of measurement. Catheter pressures in pairwise recordings (tip/port sensors) plus ECG. Flows are reconstructed into characteristic time series (CTS) from 30 MRI slices by use of ECG sync. About time gaps of measurements, see text. *Right:* segmentation (red) of end-diastolic 3D geometry of aorta for parameterization of lumped segments of aorta. Generic reconstruction of fitted segments (x,y,z,r) by use of cubic spline interpolation (yellow) is shown in overlay with STL (salmon pink) derived from clinical data. (For interpretation of the references to colour in this figure legend, the reader is referred to the web version of this article.)

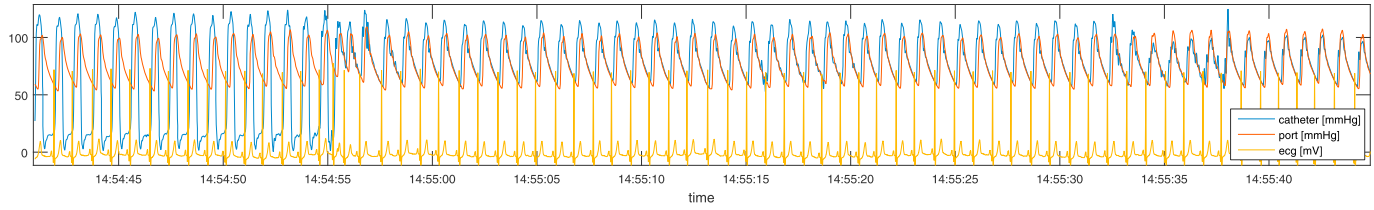

Fig. 11. Invasive pre-treatment pressures. The graph shows the full recording with catheter tip sensor being moved bit by bit from left ventricle over aorta ascending and aortic arc through the coarctation to aorta descending and reveals the significant pressure drop at the stenosis around time stamp 14:55:33.

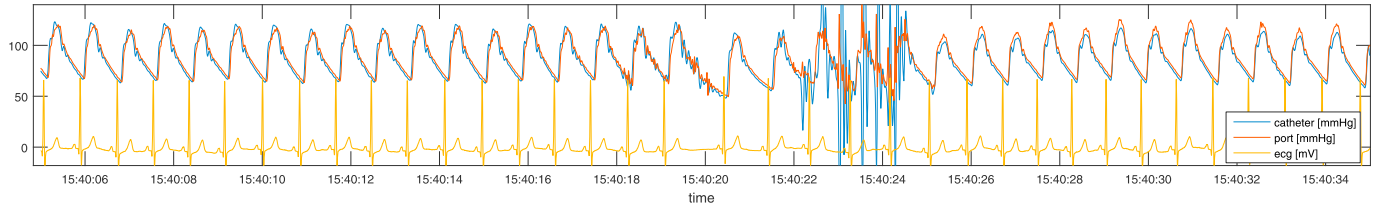

Fig. 12. Invasive post-treatment pressures after stent implantation. The record shows the catheter tip sensor initially situated at aorta ascending and then moved through the stent to aorta descending. No significant pressure difference is visible anymore.

2. **Globally remap geometric parameters (d, h, l) of the model using a prior** that factors in important metadata: In lack of a prior accounting for body height, age, gender, weight and known geometric abnormalities, a simple linear scaling with the body height coefficient (148/175) was conducted.
3. **Exploit available geometrical data to achieve a patient specific segmentation and fitting** of parameters at prominent locations, which are sensitive, pathologic, or of specific interest: Main aortic geometry and segmentation was fitted on the base of a surface map (STL) of the end-diastolic geometry as shown in Fig. 10, right. Further, parameters d, h of secondary branches coupled with main aortic structure were slightly adapted to smoothen transitions.
4. **Identify and extract periods in pressure record for use as characteristic periods** for BC and observation in simulation: Due to the lack of precise location information, a good representative pair for ASC and DESC had to be chosen by estimation, shown in Fig. 13, left. Synchronization information was extracted from ECG signal and periods were adjusted to allow for periodic and autocorrelative use.

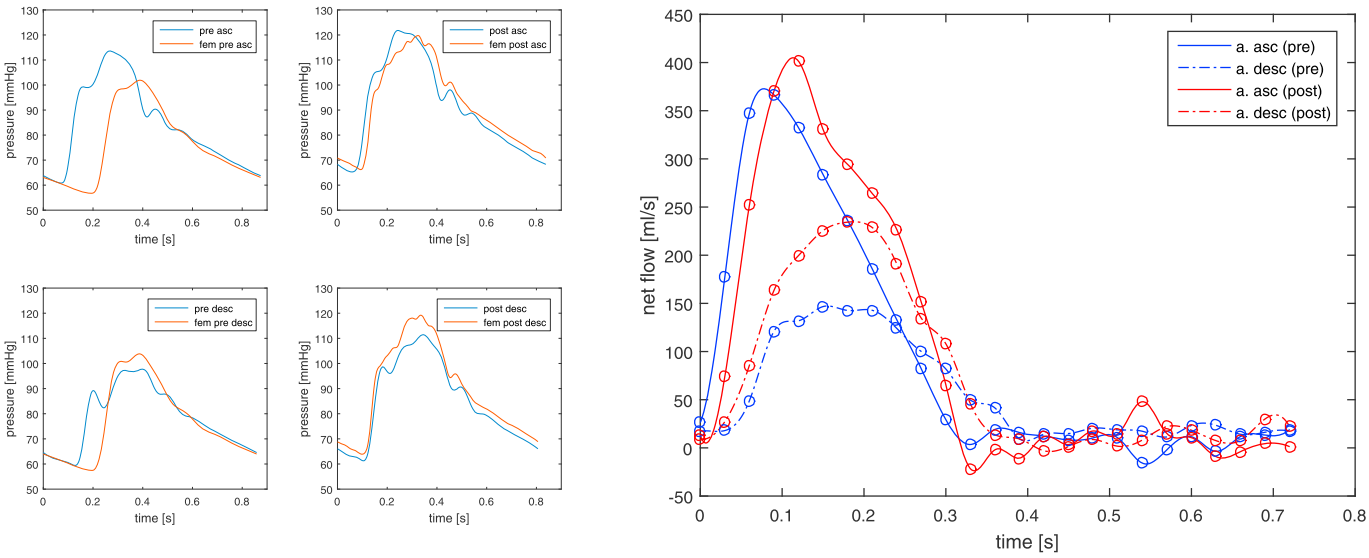

Fig. 13. *Left:* characteristic pressure periods extracted from catheter measurements in aorta ascending and aorta descending before and after stent implantation (synchronization via ECG). *Right:* MRI-derived characteristic flow periods recorded two months pre and six months post treatment. During the MRI sessions, systolic/diastolic pressures were taken (see Table 2).

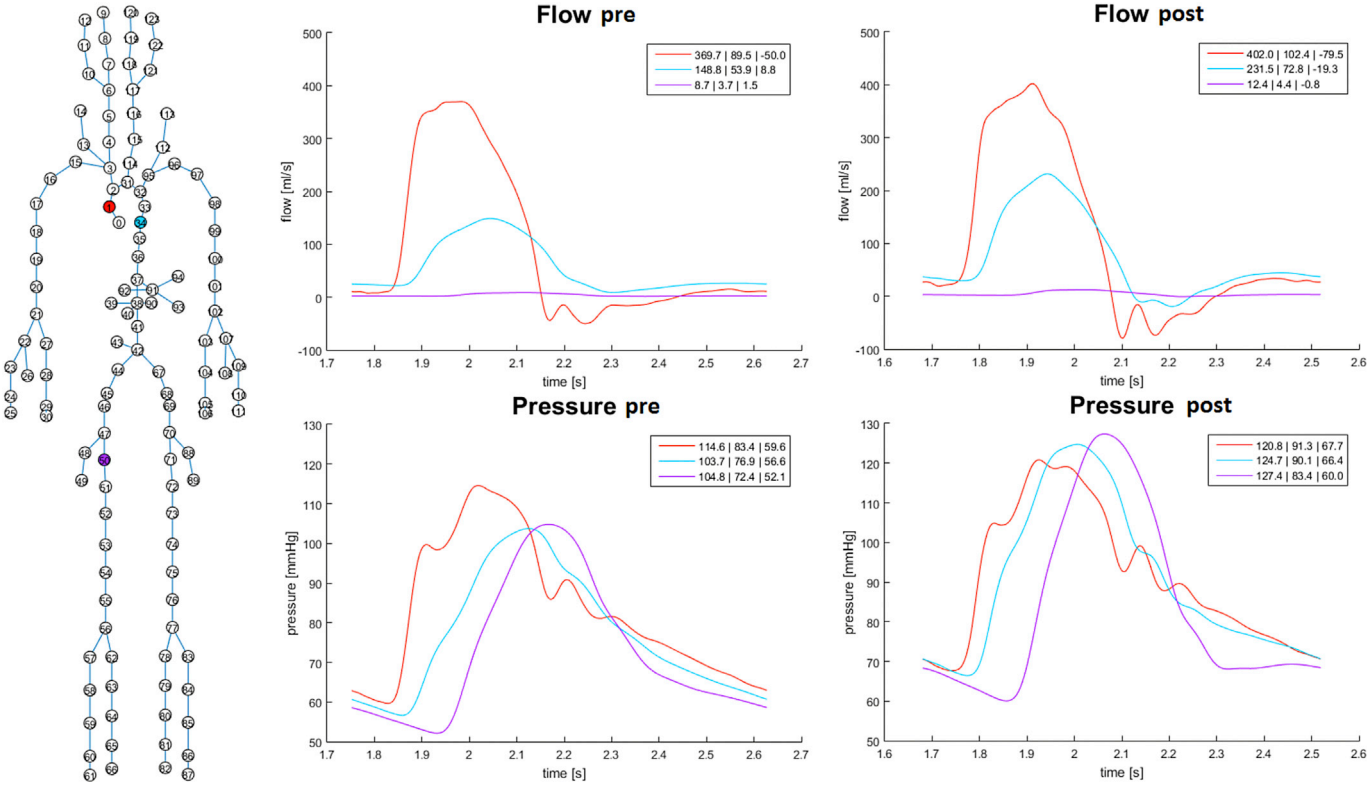

Fig. 14. CoA data modeled as pre and post scenario with visco-elastic Maxwell WKE (Fig. 3) in SISCA. Simulation runs shown were generated with aortic (asc.) pressures applied as ingoing BC (Fig. 13) at root node. General fitting was done by a geometric rescaling of a validated model and adjustment of boundary resistances (mean flows) and Young modulus (max flows). Stenosis was modeled by change of diameter and elastic modulus of stenosed segments (32, 33).

Please note that with reliable RR values gained by cuff measurements in same or comparable system condition, it can be tried to adjust pressure curves to match systoles and diastoles with a prior that introduces a suitable pressure profile for the distanced measurement points.

5. **Fit systemic resistance to adjust mean flow at known locations:** With no other flow information available, post-treatment flows were used for fitting of flow, despite the large time gap. Fitting was done by rescaling the boundary resistances of all outlets subject to a suitable weighing scheme or prior. Due to the lack of such a prior, a split linear scaling was conducted subject to ASC/DESC mean flow ratio.
6. **Fit systemic compliance to mirror max flows at known locations**: Fitting was done by reweighing the elastic modulus of all compartments with respect to a prior. As such a prior was lacking, a split linear scaling was conducted in aortic subtrees subject to ASC/DESC max flow ratio. A further optimization criterion can be gained from RR values (left/right upper lower symmetry).

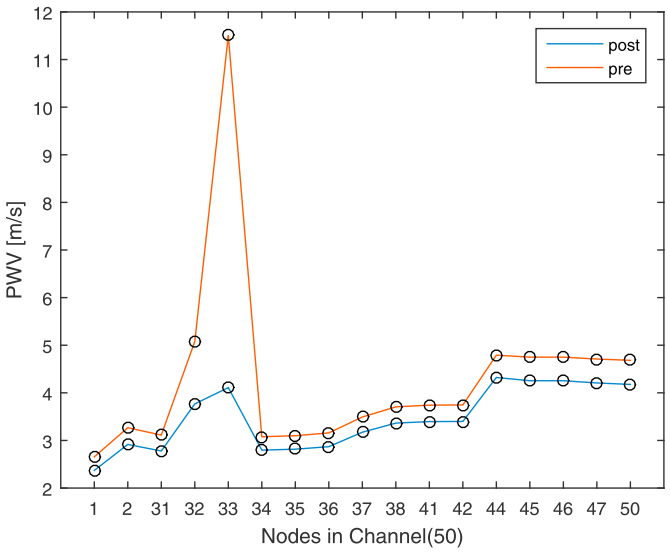

Fig. 15. Pulse wave velocities in arteries between aorta asc. and femoralis (node 50) for the two scenarios shown in Fig. 14. Calculation was done along [7] and values of unstenosed segments are in good accordance with [22].

Table 2
Cuff pressures taken during MRI sessions 57 days before treatment and 6 months after treatment.

Cuff pressures	pre treatment (syst./diast. [mmHg])	post treatment (syst./diast. [mmHg])
left arm (RR)	130/65	147/69
right arm (RR)	153/57	145/68
left leg (RR)	107/55	135/61
right leg (RR)	121/49	142/67

Table 3
Net flows taken during MRI sessions 57 days pre and 6 months post-treatment.

MRI net flows	Pre-treatment (57 days)		Post-treatment (6 months)	
	max/mean [ml/s]	$c_{aa/ad}$	max/mean [ml/s],	$c_{aa/ad}$
Aorta asc.	366/92	2.5/1.7	401/101	1.7/1.4
Aorta desc.	146/54		234/72	

7. **Fit viscous parameters to account for systemic damping and pressure levels:** With flows having been fitted, systolic pressures at known locations can be fitted by adjusting blood viscosity and viscoelastic parameters of WKE subject to suitable priors. With (reliable) RR values known, systolic pressures can be adjusted at cuff measurement points.

Any of the mentioned fitting tasks may be automated by applying some (even basic) estimation scheme in an iterative sequential or a combined fashion. As pointed out in section 4.1.3, the "best fit" of a multi-objective optimization problem will always be strongly related to how the cost function is composed and how the single objectives are weighted. Further, any weighing will result from the uncertainty model being used to attribute relevance to the individual measurement and session within the clinical data set and can lead to quite fuzzy results when conflicting information has to be accounted for.

Having fitted the model so that the result set of a simulation run reflects the post-treatment data set well, it can be used as a prior for modeling the pathologic pre-treatment state.

8. **Apply stenosis model to affected compartments (if available, according to geometrical data):** In lack of a lumped model specifically derived to account for stenosis, CoA-modeling was conducted by adjusting parameters d, h, E of the stenosed segments (nodes 32, 33), so that the ASC/DESC pressure drop was reproduced with respect to the pulse wave velocity increase by factor 4. The velocity profile of the artery channel between ASC and FEM resulting from the pre- and post-treatment parameterizations of the full model are shown in Fig. 15.
9. **Adjust and rebalance pre-treatment mean and max flows (see steps 5 and 6):** With no other flow information available, this step was conducted with pre-treatment flows, despite the long time gap.

4.1.3.2. With lumped heart model. Having identified the main system, some heart parameters can also be identified for conducting PV-loop analysis and after-load calculation on a simulation basis to gain further insight into the operation mode of the system and some validation for the parameterization of the main system. For this, a lumped heart element at the root of the arterial tree is included into the low or high-detail, multi-compartment model discussed in the previous section.[14] Methods, possible setups and related tasks are briefly sketched here:

1. **Open loop heart simulation with two-compartment model**: For bilateral flow coupling, set up a simple model comprising a lumped heart element (Fig. 3, bottom left) and a qq-flavor (Fig. 16, bottom left) modeling the valve duct until ASC only. At BC, apply constant mean or profiled synthetic flow at heart inlet (left atrium) and characteristic ASC flow periodically at outlet (Fig. 13, right). For pressure coupling at ASC, model valve duct until ASC with pq-flavor instead, then apply characteristic ASC pressures at outlet. Identify timing and parameterization of heart elastance function using LV pressures as observation.
2. **Open loop heart/aortic simulation with multi-compartment model**: For identification of aortic compliance and stenosis, extend the simple two-compartment model into a multi-compartment model with outlet at DESC (Fig. 5, bottom left) and parameterize the compartments with geometrical data (Fig. 10) and elastic modulus priors. Apply constant mean or profiled synthetic flow at inlet of heart element left atrium and characteristic ASC flow or ASC pressure at outlet (Fig. 13) periodically at DESC compartment. Identify i) diameter at stenosed compartment and ii) elastic modulus of aortic compartments using a prior distribution or areal compliances, if available.
3. **Closed loop heart/aortic/body simulation**: Use any suitable multi-compartment model containing a lumped heart element and, with no BC required, apply all measurements, including LV, ASC and DESC pressures and flows as observations (Fig. 5, bottom right). Re-identify parametrization of heart elastance function and aorta parts.
4. **Half open loop heart/aortic/body simulation:** In this scenario the closed loop setup from the previous section "Closed loop heart/aortic/body simulation" is used, but one or more pressures or flows are applied as BC to the related compartment inlets or outlets, each superseding the affected internal coupling to the predecessor or successor compartment respectively (see section 0).

For each of the mentioned scenarios, specific estimation schemes have to be selected, weighed and validated. Then continue with variational analysis using distributions calculated by the uncertainty model.

5. Results

SISCA has been successfully used to setup and identify patient specific models for the presented CoA case along the presented procedures and to reconstruct pre and post-treatment scenarios characterized by available routine clinical data sets. After interactive structure modeling and

[14] The designer component of SISCA offers some convenient copy & paste functionality to facilitate this task.

parameter tuning, automated fitting procedures were applied to the models to achieve selected optimization goals for pre and post-treatment conditioning.

Fig. 15 shows a pair of simulation results (pressures and flows for ASC, DESC and FEM) obtained for a weighed selection of pre and post-treatment conditions. Simulation was done using a high-detail, multi-compartment, patient specific model comprising visco-elastic Maxwell WKE. As pressure BC for inlet, characteristic periods (Fig. 13, left) were extracted and conditioned from the invasive catheter measurements in the clinical data set at some location that could be (vaguely) attributed to ASC (Figs. 12 and 13).

To obtain at least a reasonable conditioning and balancing of systemic resistances and compliances, the max and mean flows at ASC and DESC were used in the cost function, neglecting any time gaps and different physiological conditions (see Table 1). However, because of the large systolic pressure differences between invasive and cuff-pressures (Table 3), RR-pressures had to be disregarded.

With systemic resistances and compliances being fitted proximal and distal to the stenosis (segments 32, 33), the simulated flows mirror the measurements (Fig. 13, right) quite well. For both scenarios, specific parameterization was applied to segments 32 and 33 so that systoles at ASC and DESC were correctly simulated and stenosis and stent treatment were adequately reflected. Thus, the pressure amplitudes are also correctly reproduced by the simulation. For the arterial channel between ASC and FEM, a realistic pulse wave velocity profile was calculated along [7]. It reflects an increase of velocity by factor four at the stenosis, which is the expected behavior, as shown in Fig. 15.

When a pulse wave travels through an arterial channel, a phase shift occurs that depends on the wave velocity. In the pre-treatment data set (Fig. 13, left), a large phase shift of the pulse wave can be observed between ASC and DESC, which is typical for a stenosed arterial channel and fairly well reproduced by the simulation. However, in the post-treatment data set, this phase shift is almost completely gone. While a significant decrease of phase shift between ASC and DESC is the expected behavior after stent implementation and is also reproduced by the simulation in a reasonable amount, it seems unrealistic that almost no, or even a negative phase shift occurs within the arterial channel between ASC and FEM. In simulation, this can only be reproduced by reducing the compliance of the regarded arterial channel to unrealistic values. Effects like this might be explained with specific systemic or measurement conditions that occurred during surgery and have to be covered by uncertainty modeling.

6. Discussion and future work

Multi-compartment lumped models based on the generalized framework of Windkessel models provide a versatile approach to describe the cardiovascular system as a whole, as well as in specific parts and for specific scenarios with measured data available. Offering excellent structural freedom, they use a readily comprehensible and fairly well identifiable set of mainly geometric-based parameters and their state variables are measureable quantities. In combination with system identification and parameter estimation procedures that can operate over heterogeneous multi-point measurements, they may be utilized to generate patient specific models upon data extracted from routine clinical data.

To be able to profit from all this versatility and structural freedom, a software tool is needed that not only automates the tedious parts of the workflows connected with data conditioning, structural modeling, state space system inferring and parameter management, but also can be used to gain fast interactive simulation results for a large variety of use cases. The component based software framework SISCA presented in this paper, is such a tool.

SISCA is constantly maintained, expanded and adopted to the needs of the scientist groups that currently use it for research. Its next major revision will specifically i) address multi-graining and interfacing with other model types (1D and 3D models, organ models) and data stock, ii) seamlessly enlarge the solver suite with 1D-solvers and special purpose solvers for interfacing and iii) add uncertainty management and its integration into the variational statistics engine.

While patient specific modeling heavily depends on an effective and highly versatile modeling process, the methods and results presented in this paper also suggest that the conditioning and uncertainty management of routine clinical data sets open a wide and important area for future research.

Conflict of interest

None Declared.

Acknowledgements

Research and software development was supported by the BMBF project KF2698702KJ1. All clinical data presented in the paper were provided by Charité Universitätsmedizin (university hospital) Berlin.

Appendix A

Windkessel elements (W4S)

With this appendix we give a short introduction to Windkessel elements, specifically to those of type W4S.

Windkessel models are zero-dimensional, i.e. due to previous integration they do not contain spatial terms any more. Utilizing the hydraulic-electric analogy, they are well understood from electric network theory. Being describable as linear ODE systems, typical scenarios for numerical simulation have low computational effort, e.g. when the transfer function approach or a direct integration scheme based on the matrix exponential is used.

To derive Windkessel elements or related lumped models from the Navier-Stokes equations, several simplification assumptions have to be made. Besides a uniform circular cross-section along the length l of the segment, the elastic properties are also assumed as uniform. The fluid is assumed to be Newtonian and for simplicity, a flow profile derived for laminar and stationary flow conditions is applied. A more exhaustive mathematical derivation can be found, e.g. in Refs. [2,18]. For the linear elastic W4S shown in Fig. 16, top right, the following description of pressure p and flow q in form of a linear ODE-System is obtained [20]:

$$\dot{q} = -\frac{R}{L}q + \frac{p_{in} - p_{out}}{L} \tag{11}$$

$$\dot{p} = \frac{q_{in} - q_{out}}{C}. \tag{12}$$

Parameters $R,\ C,\ L$ describe viscous friction, wall compliance and inertial effects respectively, and have their electrical counterparts in resistance,

capacity and inductance, as the variable names suggest. With respect to multi-compartment modeling it is useful to see how R, C, L are related with the vessel geometry and the fluid and wall properties:

$$R = \frac{\mu l}{\pi r^4} \tag{13}$$

$$C = \frac{3\pi r^3 (1-\sigma^2) l}{2Eh} \tag{14}$$

$$L = \frac{\rho l}{\pi r^2}, \tag{15}$$

with μ, ρ, σ, E, l, r, h denoting blood viscosity, blood density, the vessel wall's Poisson ratio, Young's modulus, vessel length, thickness and radius, respectively. It should be noted that different authors calculate compliance differently, as assumptions about wall behavior differ. Westerhof et al. [31] for instance use

$$C = \frac{3\pi r^2 \left(\frac{r}{h}+1\right)^2 l}{E\left(2\frac{r}{h}+1\right)}. \tag{16}$$

The assumption of a stationary, laminar flow through a tube with uniform cross-section leads to the well-known Hagen-Poiseuille flow. Geometric vessel tapering is neglected in the Windkessel element, but can be effectively approximated by adjusting the diameter of adjacent sections within a multi-compartment model described in more detail in section 2.2. However, it should be noted that *not* all assumptions being made for the derivation are justified by arterial wall behavior or even straight forward. First of all, the assumption of a constant Young's modulus over a large pressure range has a variety of drawbacks. While it is needed to keep the model linear in favor of fast forward simulations, the downside is that it introduces an implicit pressure range constraint, thus harming the model's predictive power for different pressure levels severely. Obviously this issue can only be addressed with a non-linear extension of the Windkessel model that at least introduces a pressure-dependent compliance C_p (also see Refs. [14,15]).

Appendix B

WKE flavors

Depending on whether pressure or/and flow boundary conditions will be applied at inlet[15] and outlet of a WKE, model derivation (see Ref. [20]) leads to four different electrical networks (and ODE systems) as shown in Fig. 16. We call them *flavors* and notate them by using a prefix that abbreviates the BC applied at inlet and outlet. Thus, a pq-flavor is a system to which a pressure BC is applied at inlet and a flow BC at outlet.

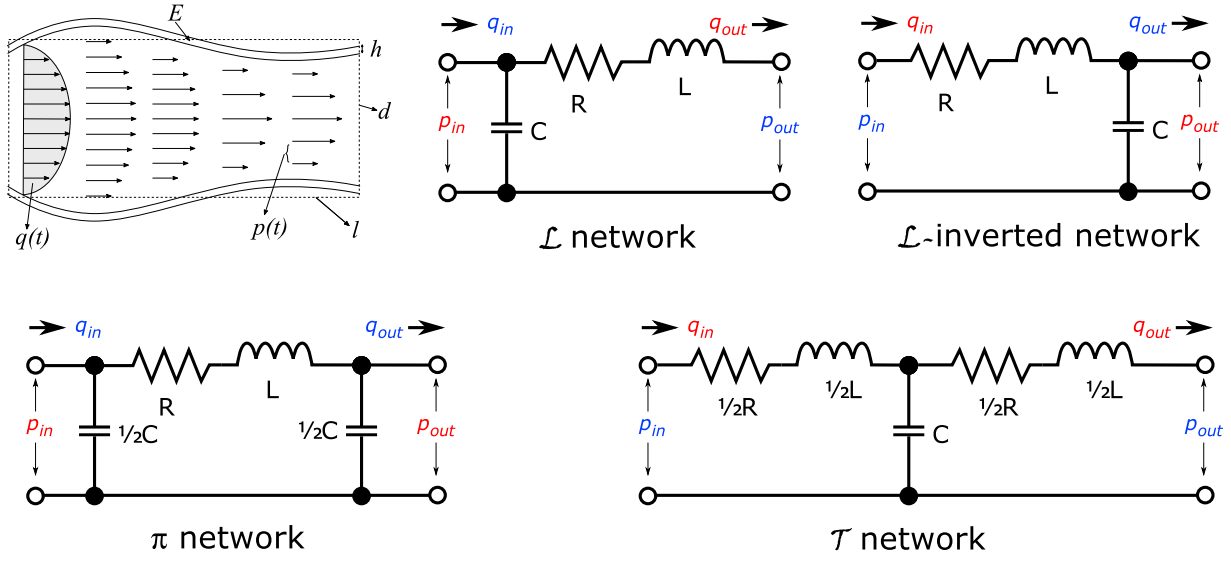

Fig. 16. Hydraulic-electric analogy and flavors of a linear elastic WKE with W4S scheme. *Top left:* idealized physical vessel segment represented with parameters E, l, d, h and state variables $q(t)$ and $p(t)$, describing flow and pressure; *top middle and right:* basic linear elastic WKE set up as electrical L and L-inverted networks; *bottom left and right*: adapter WKE set up as electrical T and π networks. Red variables are calculated, blue variables are applied as boundary conditions [20].

[15] "Inlet" and "outlet" are related to the main flow direction. Other authors [20] instead use "proximal" and "distal" to underline the loss of locality in the context of lumped models.

For the pq-flavor of the linear elastic WKE shown in Fig. 16, top right, and characterized by the equation system (11), (12) the two state space matrices A, B to be used in the state space representation equation (1) are derived as

$$A = \begin{pmatrix} -\frac{R}{L} & -\frac{1}{L} \\ \frac{1}{C} & 0 \end{pmatrix}, \; B = \begin{pmatrix} \frac{1}{L} & 0 \\ 0 & -\frac{1}{C} \end{pmatrix}, \tag{17}$$

where the state variable x describes the vector $[q_{in},\ p_{out}]^T$ and the control variable u prescribes the vector $[p_{in},\ q_{out}]^T$. The analogous derivation for the WKE's qp-flavor shown in Fig. 16, top middle, yields

$$A = \begin{pmatrix} 0 & -\frac{1}{C} \\ \frac{1}{L} & -\frac{R}{L} \end{pmatrix}, \; B = \begin{pmatrix} \frac{1}{C} & 0 \\ 0 & -\frac{1}{L} \end{pmatrix}, \tag{18}$$

where x describes $[p_{in},\ q_{out}]^T$ and u prescribes $[q_{in},\ p_{out}]^T$. For the (symmetric) pp-flavor shown in Fig. 16, bottom right, one obtains

$$A = \begin{pmatrix} -\frac{R}{L} & -\frac{2}{L} & 0 \\ \frac{1}{C} & 0 & -\frac{1}{C} \\ 0 & \frac{2}{L} & -\frac{R}{L} \end{pmatrix}, \; B = \begin{pmatrix} \frac{2}{L} & 0 \\ 0 & 0 \\ 0 & -\frac{2}{L} \end{pmatrix}, \tag{19}$$

where x describes $[q_{in},\ p,\ q_{out}]^T$ and u prescribes $[p_{in},\ p_{out}]^T$. Finally, the (symmetric) qq-flavor shown in Fig. 16, bottom left, derives to

$$A = \begin{pmatrix} 0 & -\frac{2}{C} & 0 \\ \frac{1}{L} & -\frac{R}{L} & -\frac{1}{L} \\ 0 & \frac{2}{C} & 0 \end{pmatrix}, \; B = \begin{pmatrix} \frac{2}{C} & 0 \\ 0 & 0 \\ 0 & -\frac{2}{C} \end{pmatrix}, \tag{20}$$

where x describes $[p_{in},\ q,\ p_{out}]^T$ and u prescribes $[q_{in},\ q_{out}]^T$.

References

[1] J. Alastruey, K.H. Parker, S.J. Sherwin, Arterial pulse wave haemodynamics, in: S. Anderson (Ed.), 11th International Conference on Pressure Surges, Virtual PiE Led t/a BHR Group, 2012, pp. 401–442. Chapter 7, 2012.

[2] A.J. Arimon, Numerical Modelling of Pulse Wave Propagation in the Cardiovascular System: Development, Validation and Clinical Applications PhD Thesis, Imperial College London, 2006, 2006.

[3] T. Arts, T. Delhaas, P. Bovendeerd, X. Verbeek, F.W. Prinzen, Adaptation to mechanical load determines shape and properties of heart and circulation, the CircAdapt model, Am. J. Physiol. Heart Circ. Physiol. 288 (2005) 1943–1954, 2005.

[4] T. Arts, T. Delhaas, P. Bovendeerd, X. Verbeek, F.W. Prinzen, Adaptation to mechanical load determines shape and properties of heart and circulation, the CircAdapt model, Am. J. Physiol. Heart Circ. Physiol. 288 (2005) 1943–1954, 2005.

[5] S. Bernhard, C. Al Zoukra, C. Schütte, Statistical parameter estimation and signal classification in cardiovascular diagnosis, 2011 Jul, Med. Eng. Phys. 33 (6) (2011) 739–754, http://dx.doi.org/10.2495/EHR110401. Conference: WIT Transactions on Biomedicine and Health, Vol 15.

[6] E. Butterworth, B.E. Jardine, G.M. Raymond, M.L. Neal, J.B. Bassingthwaighte, JSim, an open-source modeling system for data analysis, F1000Res. 2 (288) (2014) 19, http://dx.doi.org/10.12688/f1000research.2-288.v3, 2014.

[7] I. Cap, K. Capova, Electromagnetic modeling of blood flow in vessels, 2010, Int. J. Appl. Electromagn. Mech. 33 (2010) 735–742, http://dx.doi.org/10.3233/JAE-2010-1180. IOS Press.

[8] A. Ferreira, et al., A nonlinear state-space model of a combined cardiovascular system and a rotary pump, in: Proc. of the 44th IEEE Conference on Decision and Control, 2005. December 12-15, 2005.

[9] O. Frank, Die Grundform des arteriellen pulses, Z Biol. 37 (1899) 483–526.

[10] R. Gul, Mathematical Modeling and Sensitivity Analysis of Lumped-parameter Model of the Human Cardiovascular System, PhD thesis, FU Berlin, 2016, 2016.

[11] R. Gul, S. Bernhard, Parametric uncertainty and global sensitivity analysis in a model of the carotid bifurcation: identification and ranking of most sensitive model parameters, Math. Biosci. 269 (2015) 104–116, 2015.

[12] R. Gul, C. Schütte, S. Bernhard, Mathematical modeling and sensitivity analysis of arterial anastomosis in arm arteries, In Press Appl. Math. Model. (2016), http://dx.doi.org/10.1016/j.apm.2016.03.041, 2016.

[13] T. Heldt, R. Mukkamala, G.B. Moody, R.G. Mark, CVSim: an open-source cardiovascular simulator for teaching and research, Open Pacing Electrophys. Ther J 3 (2010) 45–54, 2010.

[14] A. Kopustinskas, I. Kupciunas, J. Marcinkeviciene, Estimation of arterial nonlinear compliance using ultrasound images, Electron. Ir. Elektrotech. 9 (2010) 105, 2010.

[15] J.K. Li, T. Cui, G.M. Drzewiecki, A nonlinear model of the arterial system incorporating a pressure-dependent compliance, IEEE Trans. Biomed. Eng. 37 (1990) 673–678, 1990.

[16] A. Lindinger, G. Schwedler, H.-W. Henze, Prevalence of congenital heart defects in newborns in Germany: results of the first registration year of the PAN study, Klin. Paediatr. 222 (2010) 321–326, 2010.

[17] W.E. Lorensen, H.E. Clinex, Marching cubes: a high resolution 3D surface construction algorithm, Comput. Graph 21 (1987) 163–169, 1987.

[18] Olufsen (M), Nadim A, On deriving lumped models for blood flow and pressure in the systemic arteries, Math. Biosci. Eng. 1 (1) (2004) 61–80. June 2004.

[19] D.L. Pham, C. Xu, J.L. Prince, Current methods in medical image segmentation, Annu. Rev. Biomed. Eng. 2 (2000) 315–337, 2000.

[20] A. Quarteroni, S. Ragni, A. Veneziani, Coupling between lumped and distributed models for blood flow problems, Comput. Vis. Sci. 4 (2001) 111–124, 2001.

[21] A. Quarteroni, A. Veneziani, C. Vergara, Review Geometric multiscale modeling of the cardiovascular system, between theory and practice, Comput. Methods Appl. Mech. Energy 302 (2016) 193–252, 2016.

[22] G.S. Reusz, et al., Reference values of pulse wave velocity in healthy children and teenagers, 2010 Aug, Hypertension 56 (2) (2010) 217–224, http://dx.doi.org/10.1161/HYPERTENSIONAHA.110.152686. Epub 2010 Jun 21.

[23] D.E. Schiavazzi, A. Baretta, G. Pennati, T.Y. Hsia, A.L. Marsden, Patient-specific parameter estimation in single-ventricle lumped circulation models under uncertainty, Int. J. Numer. Method Biomed. Eng. 8 (2016), http://dx.doi.org/10.1002/cnm.2799, 2016 May.

[24] P. Schlett, A. Brensing, S. Bernhard, Herz-kreislauf-simulator, MED engineering, 2012, pp. 9–10, 2012.

[25] J.A. Sethian, Level Set Methods and Fast Marching Methods: Evolving Interfaces in Computational Geometry, Fluid Mechanics, Computer Vision, and Materials Science, second ed., Cambridge University Press, Cambridge, 1999, 1999.
[26] Y. Shi, P. Lawford, R. Hose, Review of zero-D and 1-D models of blood flow in the cardiovascular system, 2011, Biomed. Eng. Online 10 (2011) 33, http://dx.doi.org/10.1186/1475-925X-10-33. Published online 2011 April 26.
[27] N. Stergiopulos, B. Westerhof, N. Westerhof, Total arterial inertance as the fourth element of the windkessel model, Am. J. Physiol. 276 (1 Pt 2) (1999) H81–H88, 1999 Jan.
[28] N. Stergiopulos, D.F. Young, T.R. Rowe, Computer simulation of arterial flow with applications to arterial and aortic stenoses, J. Biomech. 25 (12) (1992) 1477–1488, 1992.
[29] F.N. v.d. Vosse, N. Stergiopulos, Pulse wave propagation in the arterial tree, Annu. Rev. Fluid Mech. 43 (2011) 467–499, http://dx.doi.org/10.1146/annurev-fluid-122109-160730, 2011.
[30] R. v.d. Merwe, Sigma-Point Kalman Filters for Probabilistic Inference in Dynamic State-space Models, 2004 (2004). Student Scholar Archive. Paper 8.
[31] N. Westerhof, F. Bosman, S.J. de Vries, A. Noordergraaf, Analog studies of the human systemic arterial tree, J. Biomech. 2 (2) (1969) 121–143, 1969.
[32] N. Westerhof, J. Lankhaar, B.E. Westerhof, The arterial Windkessel, Med. Biol. Eng. Comput. 47 (2009) 131, http://dx.doi.org/10.1007/s11517-008-0359-2, 2009.
[33] S. Zenker, J. Rubin, G. Clermont, From inverse problems in mathematical physiology to quantitative differential diagnoses, PLoS Comput. Biol. 3 (11) (2007) e204, http://dx.doi.org/10.1371/journal.pcbi.0030204.
[34] H. Zhenghui, S. Pengcheng, Sensitivity analysis for biomedical models, IEEE Trans. Med. Imaging 29 (11) (2010) 1870–1881, 2010.